Selective Binding and Activation of One Aldehyde Enantioface by a Chiral Transition-Metal Lewis Acid: Synthesis, Structure, and Reactivity of Rhenium Aldehyde Complexes $[(\eta^5\text{-}C_5H_5)Re(NO)(PPh_3)(\eta^2\text{-}O{=}CHR)]^+X^-$

Charles M. Garner,[1a] N. Quirós Méndez,[1a] James J. Kowalczyk,[1a] Jésus M. Fernández,[1a] Kenneth Emerson,[1b] Raymond D. Larsen,[1b] and J. A. Gladysz*[,1a]

Contribution from the Departments of Chemistry, University of Utah, Salt Lake City, Utah 84112, and Montana State University, Bozeman, Montana 59717.
Received December 1, 1989

Abstract: Reaction of dichloromethane complex $[(\eta^5\text{-}C_5H_5)Re(NO)(PPh_3)(ClCH_2Cl)]^+X^-$ ($\mathbf{2}^+PF_6^-$ or $\mathbf{2}^+BF_4^-$) and RCH=O (R = (**a**) CH_3, (**b**) C_2H_5, (**c**) $n\text{-}C_3H_7$, (**d**) $i\text{-}C_3H_7$, (**e**) C_6H_5, (**f**) $CH_2C_6H_5$) gives π-aldehyde complexes (*RS,SR*)-$[(\eta^5\text{-}C_5H_5)Re(NO)(PPh_3)(\eta^2\text{-}O{=}CHR)]^+X^-$ ((*RS,SR*)-**3a-f**$^+X^-$, 98-77%), in which one RCH=O enantioface is bound with high specificity. Crystal structures of (*RS,SR*)-**3b**$^+BF_4^-$ and (*RS,SR*)-**3f**$^+PF_6^-$ show the *R*CH=O carbon to be anti to the PPh_3 ligand and the *R*CH=O group to be syn to the NO ligand. Formyl complex $(\eta^5\text{-}C_5H_5)Re(NO)(PPh_3)(CHO)$ (**5**) and (*RS,SR*)-**3a-f**$^+X^-$ react at −80 °C to give $[(\eta^5\text{-}C_5H_5)Re(NO)(PPh_3)(CO)]^+X^-$ and alkoxide complexes $(\eta^5\text{-}C_5H_5)Re(NO)(PPh_3)(OCH_2R)$ (**6a-f**, 95-80%). Reaction of deuterioformyl complex **5**-d_1 and (*RS,SR*)-**3a-f**$^+X^-$ gives deuterioalkoxide complexes $(\eta^5\text{-}C_5H_5)Re(NO)(PPh_3)(OCHDR)$ (**6a-f**-d_1) as 97-92:3-8 mixtures of (*RR,SS*)/(*RS,SR*) diastereomers. Analogous reactions starting with optically active $\mathbf{2}^+X^-$ give optically active aldehyde and alkoxide complexes with retention of configuration at rhenium. The latter react with electrophiles EX (EX = HI, $(CH_3)_3SiI$, CH_3COI) to give cleavage products $EOCH_2R$ and $(\eta^5\text{-}C_5H_5)Re(NO)(PPh_3)(X)$, generally with retention at rhenium. When (+)-(*RS*)-**3a-f**$^+BF_4^-$ are treated with (+)-(*S*)-**5**-d_1 and (−)-(*R*)-**5**-d_1, (+)-**6a-f**-d_1 form as 99-94:1-6 and 91-84:9-16 mixtures of (*RR*)/(*RS*) diastereomers, respectively. Hence, enantiomers of the chiral reductant **5**-d_1 give different stereoselectivities. Reaction of (+)-**6a-f**-d_1 with (−)-(*R*)-$C_6H_5CH(OAc)COOH$/DCC/4-(dimethylamino)pyridine gives esters $C_6H_5CH(OAc)COOCHDR$ that are comparable mixtures of (*RR*)/(*RS*) diastereomers and carboxylate (+)-(*RR*)-$(\eta^5\text{-}C_5H_5)Re(NO)(PPh_3)(O(C{=}O)CH(OAc)C_6H_5)$ of >99% de.

The development of methodologies for the conversion of achiral aldehydes to optically active chiral alcohols has been of intense recent interest.[2-5] Procedures that are general and give high optical yields have particular value in asymmetric organic synthesis. Strategies can be classified into two broad categories: catalytic[2,3] or stoichiometric[4,5] with respect to the chiral reagent or auxiliary employed.

Organic molecules are frequently activated toward nucleophilic attack upon complexation to a transition metal.[6] Also, optically active, chiral-at-metal complexes are becoming increasingly available.[7,8] For example, we have shown that chiral rhenium complexes of the general formula $[(\eta^5\text{-}C_5R_5)Re(NO)(PPh_3)(L)]^{n+}$ are readily obtained in optically pure form[8] and undergo diverse types of ligand and metal-based transformations with high stereoselectivity.[9] Hence, we sought to synthesize and probe the chemistry of the corresponding rhenium aldehyde complexes.[10]

Scheme I. Syntheses of Aldehyde Complexes (*RS,SR*)-$[(\eta^5\text{-}C_5H_5)Re(NO)(PPh_3)(\eta^2\text{-}O{=}CHR)]^+X^-$ ((*RS,SR*)-**3**$^+X^-$)

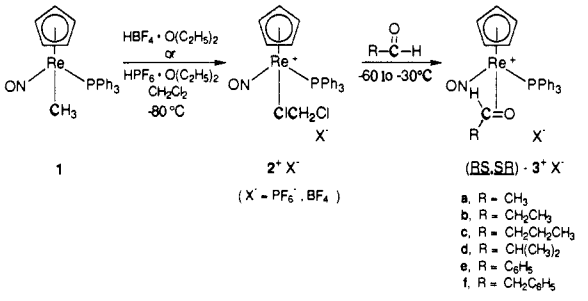

(1) (a) University of Utah. (b) Montana State University.

(2) Asymmetric additions of zinc alkyls catalyzed by chiral amines: (a) Kitamura, M.; Okada, S.; Suga, S.; Noyori, R. *J. Am. Chem. Soc.* **1989**, *111*, 4028. (b) Soai, K.; Watanabe, M.; Koyano, M. *J. Chem. Soc., Chem. Commun.* **1989**, 534. (c) Noyori, R.; Suga, S.; Kawai, K.; Okada, S.; Kitamura, M.; Oguni, N.; Hayashi, M.; Kaneko, T.; Matsuda, Y. *J. Organomet. Chem.* **1990**, *382*, 19. (d) References contained in the preceding articles.

(3) Asymmetric aldol reactions catalyzed by a chiral Fe/Au complex: (a) Ito, Y.; Sawamura, M.; Hayashi, T. *J. Am. Chem. Soc.* **1986**, *108*, 6405. (b) Ito, Y.; Sawamura, M.; Hamashima, H.; Emura, T.; Hayashi, T. *Tetrahedron Lett.* **1989**, *30*, 4681. (c) Pastor, S. D.; Togni, A. *J. Am. Chem. Soc.* **1989**, *111*, 2333. (d) Togni, A.; Pastor, S. D. *J. Org. Chem.* **1990**, *55*, 1649.

(4) Representative asymmetric aldehyde reductions that employ stoichiometric quantities of the chiral reagent or auxiliary: (a) Mukaiyama, T.; Soai, K.; Sato, T.; Shimizu, H.; Suzuki, K. *J. Am. Chem. Soc.* **1979**, *101*, 1455. (b) Mazaleyrat, J.-P.; Cram, D. J. *Ibid.* **1981**, *103*, 4585. (c) Noyori, R.; Tomino, I.; Yamada, M.; Nishizawa, M. *Ibid.* **1984**, *106*, 6717. (d) Weidmann, B.; Seebach, D. *Angew. Chem., Int. Ed. Engl.* **1983**, *22*, 31, see pp 39 and 40. (e) Midland, M. M. *Chem. Rev.* **1989**, *89*, 1553. (f) Short, R. P.; Masamune, S. *J. Am. Chem. Soc.* **1989**, *111*, 1892 and references therein. (g) Corey, E. J.; Imwinkelried, R.; Pikul, S.; Xiang, Y. B. *Ibid.* **1989**, *111*, 5493. (h) A recently reported chiral catalyst: Corey, E. J.; Link, J. O. *Tetrahedron Lett.* **1989**, *30*, 6275.

(5) (a) Faller, J. W.; Linebarrier, D. L. *J. Am. Chem. Soc.* **1989**, *111*, 1937. (b) Faller, J. W.; John, J. A.; Mazzieri, M. R. *Tetrahedron Lett.* **1989**, *30*, 1769. (c) Riediker, M.; Duthaler, R. O. *Angew. Chem., Int. Ed. Engl.* **1989**, *28*, 494 and immediately following papers.

(6) (a) Collman, J. P.; Hegedus, L. S.; Norton, J. R.; Finke, R. G. *Principles and Applications of Organotransition Metal Chemistry*; University Science Books: Mill Valley, CA; Chapter 7. (b) Eisenstein, O.; Hoffmann, R. *J. Am. Chem. Soc.* **1981**, *103*, 4308. (c) Cameron, A. D.; Smith, V. H., Jr.; Baird, M. C. *J. Chem. Soc., Dalton Trans.* **1988**, 1037.

(7) (a) Brunner, H. *Adv. Organomet. Chem.* **1980**, *18*, 151. (b) Flood, T. C.; Campbell, K. D.; Downs, H. H.; Nakanishi, S. *Organometallics* **1983**, *2*, 1590. (c) Faller, J. W.; Chao, K.-H. *Ibid.* **1984**, *3*, 927. (d) Consiglio, G.; Morandini, F. *Chem. Rev.* **1987**, *87*, 761. (e) Hommelsoft, S. I.; Baird, M. C. *Organometallics* **1986**, *5*, 1380. (f) Davies, S. G.; Dordor-Hedgecock, I. M.; Sutton, K. H.; Walker, J. C.; Bourne, C.; Jones, R. H.; Prout, K. *J. Chem. Soc., Chem. Commun.* **1986**, 607. (g) Brookhart, M.; Liu, Y. *Organometallics* **1989**, *8*, 1572.

(8) (a) Merrifield, J. H.; Strouse, C. E.; Gladysz, J. A. *Organometallics* **1982**, *1*, 1204. (b) Huang, Y.-H.; Niedercorn, F.; Arif, A. M.; Gladysz, J. A. *J. Organomet. Chem.* **1990**, *383*, 213.

(9) Some lead references: (a) Merrifield, J. H.; Lin, G.-Y.; Kiel, W. A.; Gladysz, J. A. *J. Am. Chem. Soc.* **1983**, *105*, 5811. (b) O'Connor, E. J.; Kobayashi, M.; Floss, H. G.; Gladysz, J. A. *Ibid.* **1987**, *109*, 4837. (c) Bodner, G. S.; Smith, D. E.; Hatton, W. G.; Heah, P. C.; Rheingold, A. L.; Geib, S. J.; Hutchinson, J. P.; Gladysz, J. A. *Ibid.* **1987**, *109*, 7688. (d) Senn, D. R.; Wong, A.; Patton, A. T.; Marsi, M.; Strouse, C. E.; Gladysz, J. A. *Ibid.* **1988**, *110*, 6096. (e) Crocco, G. L.; Lee, K. E.; Gladysz, J. A. Submitted for publication. (f) Zwick, B. D.; Arif, A. M.; Patton, A. T.; Gladysz, J. A. *Angew. Chem., Int. Ed. Engl.* **1987**, *26*, 910.

(10) Review of aldehyde and ketone complexes: Huang, Y.-H.; Gladysz, J. A. *J. Chem. Educ.* **1988**, *65*, 298.

0002-7863/90/1512-5146$02.50/0

Table I. Spectroscopic Characterization of Aldehyde Complexes (*RS,SR*)-$[(\eta^5\text{-}C_5H_5)Re(NO)(PPh_3)(\eta^2\text{-}O{=}CHR)]^+PF_6^-$ ((*RS,SR*)-**3**$^+PF_6^-$)

complex (R)	IR ν_{NO},[a] cm^{-1}	^1H NMR,[b] δ	$^{13}C\{^1H\}$ NMR,[c] ppm	$^{31}P\{^1H\}$ NMR,[d] ppm
(*RS,SR*)-**3a**$^+PF_6^-$ (CH_3)	1737 (vs)	7.63–7.33 (m, 3 C_6H_5), 5.83 (s, C_5H_5), 5.50 (m, HCO), 2.32 (d, J = 4.0, CH_3)	PPh_3 at[e] 133.8 (d, J = 10.6, *o*), 133.1 (d, J = 2.9, *p*), 129.9 (d, J = 11.5, *m*), 127.6 (d, J = 59.8, *i*); 98.8 (s, C_5H_5), 79.5 (s, CO), 24.6 (s, CH_3)	10.0 (s)
(*RS,SR*)-**3b**$^+PF_6^-$ (CH_2CH_3)	1738 (vs)	7.67–7.42 (m, 3 C_6H_5), 5.96 (d, J_{PH} = 0.5, C_5H_5), 5.44 (ddd, J = 5.4, 4.2, J_{PH} = 2.3, HCO), 2.88 (dddq, J = 14.5, 7.4, 4.2, J_{PH} = 0.7, C*H*H′), 1.95 (ddq, J = 14.5, 7.5, 5.5, CH*H*′), 1.24 (t, J = 7.5, CH_3)	PPh_3 at 133.6 (d, J = 10.4, *o*), 133.0 (d, J = 2.6, *p*), 129.8 (d, J = 11.4, *m*), 127.4 (d, J = 59.5, *i*); 98.5 (s, C_5H_5), 85.8 (br s, CO), 32.5 (s, CH_2), 13.2 (s, CH_3)	10.0 (s)
(*RS,SR*)-**3c**$^+PF_6^-$ ($CH_2CH_2CH_3$)	1740 (vs)	7.67–7.42 (m, 3 C_6H_5), 5.92 (s, C_5H_5), 5.37 (ddd, J = 4.4, 5.2, J_{PH} = 2.3, HCO), 2.42 (m, C*H*H′), 2.12 (m, CH*H*′), 1.67 (m, CH_2), 1.02 (t, J = 7.3, CH_3)	PPh_3 at 133.5 (d, J = 9.6, *o*), 133.0 (d, J = 2.2, *p*), 129.8 (d, J = 11.5, *m*), 127.3 (d, J = 60.3, *i*); 98.3 (s, C_5H_5), 83.3 (br s, CO), 41.1 (s, CH_2), 23.6 (s, CH_2CH_3), 14.2 (s, CH_3)	10.1 (s)
(*RS,SR*)-**3d**$^+PF_6^-$ ($CH(CH_3)_2$)	1740 (vs)	7.67–7.42 (m, 3 C_6H_5), 5.96 (d, J_{PH} = 0.5, C_5H_5), 5.19 (dd, J = 7.2, J_{PH} = 2.3, HCO), 1.68 (pseudooctet, J = 6.8, C*H*-$(CH_3)_2$), 1.33 (d, J = 6.6, CH_3), 1.17 (d, J = 6.8, CH_3′)	PPh_3 at 133.6 (d, J = 10.4, *o*), 133.0 (d, J = 2.8, *p*), 129.8 (d, J = 10.5, *m*), 127.3 (d, J = 59.9, *i*); 98.5 (s, C_5H_5), 89.0 (br s, CO), 38.2 (s, CH), 25.2 (s, CH_3), 19.5 (s, CH_3′)	10.0 (s)
(*RS,SR*)-**3e**$^+PF_6^-$ (C_6H_5)	1735 (vs)	7.90–7.06 (m, 4 C_6H_5), 6.81 (d, J_{PH} = 1.4, HCO), 5.89 (s, C_5H_5)	PPh_3 at[e] 134.0 (d, J = 10.2, *o*), 133.1 (s, *p*), 130.0 (d, J = 11.2, *m*), 127.9 (d, J = 59.1, *i*); CPh at 139.5 (s, *i*), 130.7 (s), 128.7 (s), 127.1 (s); 99.3 (s, C_5H_5), 89.5 (br s, CO)	10.0 (s)
(*RS,SR*)-**3f**$^+PF_6^-$ ($CH_2C_6H_5$)	1729 (vs)	7.71–7.27 (m, 4 C_6H_5), 5.84 (s, C_5H_5), 5.44 (br m, HCO), 3.58 (dd, J = 14.2, 5.8, C*H*H′), 3.44 (dd, J = 14.2, 3.9, CH*H*′)[f]	PPh_3 at 134.1 (d, J = 10.9, *o*), 133.9 (s, *p*), 130.5 (d, J = 11.4, *m*), 127.7 (d, J = 60.3, *i*); CPh at 139.5 (s, *i*), 129.7 (s), 129.5 (s), 128.0 (s); 99.0 (s, C_5H_5), 81.0 (br s, CO), 45.5 (s, CH_2)	10.1 (s)

[a] KBr disk. [b] Recorded at 300 MHz in CD_2Cl_2 at ambient probe temperature and referenced to internal $Si(CH_3)_4$. All couplings are in Hz. [c] Recorded at 75 MHz in CD_2Cl_2 at ambient probe temperature and referenced to CD_2Cl_2 (53.8 ppm). All couplings are in Hz and are to ^{31}P unless noted. Assignments of phenyl carbon resonances were made as described in footnote *c* of Table I in ref 19. [d] Recorded with external lock at 32.2 MHz in CD_2Cl_2 at ambient probe temperature and referenced to external 85% H_3PO_4 unless noted. [e] These spectra were obtained with (+)-(*RS*)-**3a**$^+BF_4^-$ and (+)-(*RS*)-**3e**$^+BF_4^-$. The racemates (*RS,SR*)-**3a,e**$^+X^-$ are poorly soluble in CD_2Cl_2, CD_3CN, acetone-d_6, and THF-d_8. [f] Solvate resonance at δ 5.63 (s, 0.5 CH_2Cl_2) in acetone-d_6.

We recently reported that the reaction of methyl complex $(\eta^5\text{-}C_5H_5)Re(NO)(PPh_3)(CH_3)$ (**1**) and $HBF_4{\cdot}O(C_2H_5)_2$ or $HPF_6{\cdot}O(C_2H_5)_2$ gives the labile dichloromethane complex $[(\eta^5\text{-}C_5H_5)Re(NO)(PPh_3)(ClCH_2Cl)]^+X^-$ (**2**$^+X^-$).[11] Complex **2**$^+X^-$ reacts with a variety of donor ligands (L) between −50 and −30 °C to give substitution products $[(\eta^5\text{-}C_5H_5)Re(NO)(PPh_3)(L)]^+X^-$ in high yields. When optically active **1** is utilized, these adducts are obtained in high optical yields and with overall retention of configuration at rhenium.[11] Thus, **2**$^+X^-$ serves as the functional equivalent of the chiral Lewis acid $[(\eta^5\text{-}C_5H_5)Re(NO)(PPh_3)]^+X^-$ (I). In this paper, we report (1) the conversion of racemic and optically active **2**$^+X^-$ to racemic and optically active π-aldehyde complexes $[(\eta^5\text{-}C_5H_5)Re(NO)(PPh_3)(\eta^2\text{-}O{=}CHR)]^+X^-$ (**3**$^+X^-$) in high chemical and optical yields, (2) crystallographic and spectroscopic data that show that Lewis acid I binds one aldehyde enantioface with high selectivity, (3) the reduction of **3**$^+X^-$ to racemic and optically active alkoxide complexes $(\eta^5\text{-}C_5H_5)Re(NO)(PPh_3)(OCH_2R)$ in high chemical and optical yields, (4) reactions of the optically active alkoxide complexes and electrophiles that give alcohols (or derivatives) and optically active rhenium complexes in high chemical and optical yields, (5) highly stereoselective reductions of **3**$^+BF_4^-$ to racemic and optically active deuterioalkoxide complexes $(\eta^5\text{-}C_5H_5)Re(NO)(PPh_3)(OCHDR)$, and the subsequent conversion of the optically active complexes to esters of optically active deuterioalcohols, and (6) mechanistic analyses of the preceding transformations. A portion of this study has been communicated.[12]

Results

1. Syntheses of Aldehyde Complexes. Methyl complex $(\eta^5\text{-}C_5H_5)Re(NO)(PPh_3)(CH_3)$ (**1**)[13] and $HPF_6{\cdot}O(C_2H_5)_2$ were combined in CH_2Cl_2 at −80 °C to give dichloromethane complex $[(\eta^5\text{-}C_5H_5)Re(NO)(PPh_3)(ClCH_2Cl)]^+PF_6^-$ (**2**$^+PF_6^-$) as previously described.[11] Then 3 equiv of (**a**) acetaldehyde, (**b**) propionaldehyde, (**c**) butyraldehyde, (**d**) isobutyraldehyde, (**e**) benzaldehyde, and (**f**) phenylacetaldehyde were added. Workup gave π-aldehyde complexes (*RS,SR*)-$[(\eta^5\text{-}C_5H_5)Re(NO)(PPh_3)(\eta^2\text{-}O{=}CHR)]^+PF_6^-$ ((*RS,SR*)-**3a-f**$^+PF_6^-$)[14,15] in 91–77% yields as tan to yellow crystals or powders (Scheme I). During the course of this study, the quantity and quality of $HPF_6{\cdot}O(C_2H_5)_2$ available from commercial sources became erratic. Hence, tetrafluoroborate salts (*RS,SR*)-**3a-f**$^+BF_4^-$ were analogously prepared from **1** and $HBF_4{\cdot}O(C_2H_5)_2$. Product stereochemistry was assigned as described below.

Complexes (*RS,SR*)-**3a-f**$^+X^-$ were characterized by microanalysis (Experimental Section) and by IR and ^1H, $^{13}C\{^1H\}$, and $^{31}P\{^1H\}$ NMR spectroscopy (Table I). Spectroscopic features were characteristic of cationic $[(\eta^5\text{-}C_5H_5)Re(NO)(PPh_3)(L)]^+X^-$ complexes (IR ν_{NO}, ^{31}P NMR PPh_3 chemical shift, ^1H and ^{13}C NMR cyclopentadienyl chemical shifts). Solutions of aliphatic aldehyde complexes **3a-d**$^+X^-$ and **3f**$^+X^-$ were amber, whereas

(11) Fernández, J. M.; Gladysz, J. A. *Organometallics* **1989**, *8*, 207.
(12) Fernández, J. M.; Emerson, K.; Larsen, R. D.; Gladysz, J. A. *J. Am. Chem. Soc.* **1986**, *108*, 8268.
(13) Tam, W.; Lin, G.-Y.; Wong, W.-K.; Kiel, W. A.; Wong, V. K.; Gladysz, J. A. *J. Am. Chem. Soc.* **1982**, *104*, 141.

(14) (a) The absolute configuration at rhenium (the higher priority atom) is specified first and is assigned according to the Baird/Sloan modification of the Cahn–Ingold–Prelog priority rules. The $\eta^5\text{-}C_5H_5$ and $\eta^2\text{-}O{=}CHR$ ligands are considered pseudoatoms of atomic numbers 30 and 14, respectively, which gives the following sequence: I > $\eta^5\text{-}C_5H_5$ > PPh_3 > $\eta^2\text{-}O{=}CHR$ > OCH_2R > NO > CH_3 (Stanley, K.; Baird, M. C. *J. Am. Chem. Soc.* **1975**, *97*, 6598; Sloan, T. E. *Top. Stereochem.* **1981**, *12*, 1). (b) The configuration of the aldehyde-based stereogenic unit of **3a-f**$^+X^-$ (specified second) is assigned by the Paiaro/Panunzi convention. The complex is drawn in a metallaoxacyclopropane resonance form and the Cahn–Ingold–Prelog rules are applied to the resulting asymmetric carbon (Paiaro, G.; Panunzi, A. *J. Am. Chem. Soc.* **1964**, *88*, 5148).

(15) (a) Prefixes (+) and (−) refer to optical rotations at 589 nm. All $[\alpha]$ were measured in thermostated cells (generally 25.0 ± 0.2 °C) in CH_2Cl_2 (aldehyde complexes) or $CHCl_3$ (**6a-f**, **8**, **9**) with c = 1.0–1.3 mg/mL. (b) Since the lower crystallinity of optically active $[(\eta^5\text{-}C_5H_5)Re(NO)(PPh_3)(L)]^{n+}$ complexes can hamper purification, $[\alpha]$ is often only a rough measure of optical purity.

solutions of benzaldehyde complex $3e^+X^-$ were dark orange and noticeably thermochromic. The UV/visible spectra of these and several substituted benzaldehyde complexes will be described elsewhere.[16]

Optically active aldehyde complexes (+)-(*RS*)- and (−)-(*SR*)-**3a–f**$^+BF_4^-$ were synthesized from optically active methyl complexes (+)-(*S*)- and (−)-(*R*)-**1** by analogous procedures.[14,15] These were considerably more soluble than the racemates and were isolated as powders. Their spectroscopic properties were identical with those of the racemates, and they were further characterized by optical rotations in thermostated cells (Experimental Section).[15b] Absolute configurations, corresponding to retention at rhenium, were assigned by analogy to related transformations of optically active **1** and 2^+X^-.[11] As noted previously,[8,9a,b,f,17] the sign of $[\alpha]_{589}$ commonly correlates with the absolute configuration of optically active $[(\eta^5\text{-}C_5H_5)Re(NO)(PPh_3)(L)]^{n+}$ (n = 1, 0) complexes.

A sample of racemic benzaldehyde complex (*RS,SR*)-$3e^+BF_4^-$ was treated with the chiral NMR shift reagent, (+)-Eu(hfc)$_3$ (2.5–3.5 equiv, CD_2Cl_2). The cyclopentadienyl ^1H NMR resonances of the two enantiomers exhibited near-baseline resolution. Under analogous conditions, the cyclopentadienyl resonances of each enantiomer of propionaldehyde complex (*RS,SR*)-$3b^+BF_4^-$ exhibited half-height resolution. When the ^1H NMR spectrum of optically active benzaldehyde complex (+)-(*RS*)-$3e^+BF_4^-$ was similarly acquired in the presence of (+)-Eu(hfc)$_3$, no trace of the opposite enantiomer was observed. A detection limit of 2.5%, corresponding to ≥95% ee, was estimated.

Interestingly, the optical rotation of benzaldehyde complex (+)-(*RS*)-$3e^+BF_4^-$ was markedly dependent upon temperature: $[\alpha]_{589}$ 317° (30.8 °C), 306° (26.1 °C), 280° (14.5 °C), 269° (0.9 °C), 254° (−11 °C).[15a] When a CH_2Cl_2 solution of (+)-(*RS*)-$3e^+BF_4^-$ was kept at 32.9 °C for 13 h, $[\alpha]^{33}_{589}$ decreased from 324° to 237°. A second sample was kept at room temperature for 16 h. Subsequent (+)-Eu(hfc)$_3$ analysis indicated an optical purity of ca. 94% ee.

Optically active deuteriobenzaldehyde complex (+)-(*RS*)-$3e^+$-d_1-BF_4^- was similarly synthesized from (+)-(*S*)-**1** and benzaldehyde-d_1. Also, optically active benzaldehyde complex (+)-(*RS*)-$3e^+BF_4^-$ (0.070 M in CD_2Cl_2) was treated with 15 equiv of benzaldehyde-d_1 at 30 °C. Deuteriobenzaldehyde complex (+)-(*RS*)-$3e^+$-d_1-BF_4^- formed with $k_{obs} = 9.9 \pm 0.1 \times 10^{-5}$ s^{-1}, corresponding to a half-life of 1.9 h.[18] Hence, aldehyde ligands do not undergo particularly rapid exchange at room temperature.

2. Binding of Aldehyde Ligands: π (η^2) vs σ (η^1). The dominance of the π aldehyde coordination mode in (*RS,SR*)-3^+X^- was apparent from the following spectroscopic features:[10] (1) the absence of an IR $\nu_{C=O}$. (2) the upfield ^{13}C NMR shift of the aldehydic carbon (79–89 ppm), and (3) the upfield ^1H NMR shift of the aldehydic protons (δ 5.2–5.4 for the aliphatic aldehydes and δ 6.8 for benzaldehyde). These properties resembled those found earlier for π-formaldehyde complex $[(\eta^5\text{-}C_5H_5)Re(NO)(PPh_3)(\eta^2\text{-}O{=}CH_2)]^+PF_6^-$ (**4**$^+PF_6^-$), which was synthesized by an oxidative route.[19] However, reactions of 2^+X^- and ketones RR′C=O afford σ complexes $[(\eta^5\text{-}C_5H_5)Re(NO)(PPh_3)(\eta^1\text{-}O{=}CRR')]^+X^-$,[20] suggesting that the π and σ binding modes are close in energy.

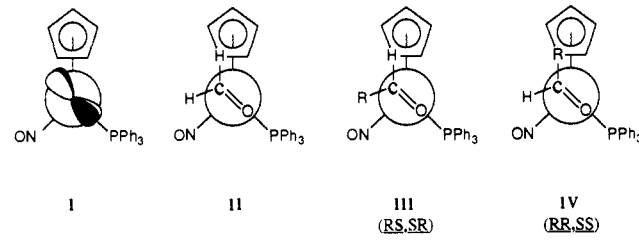

Figure 1. (I) Pyramidal rhenium fragment $[(\eta^5\text{-}C_5H_5)Re(NO)(PPh_3)]^+$ with d-orbital HOMO; (II) Newman projection of the structure of formaldehyde complex $[(\eta^5\text{-}C_5H_5)Re(NO)(PPh_3)(\eta^2\text{-}O{=}CH_2)]^+PF_6^-$ (**4**$^+PF_6^-$); (III and IV) Newman projections of possible diastereomers of substituted aldehyde complexes $[(\eta^5\text{-}C_5H_5)Re(NO)(PPh_3)(\eta^2\text{-}O{=}CHR)]^+X^-$ (3^+X^-).

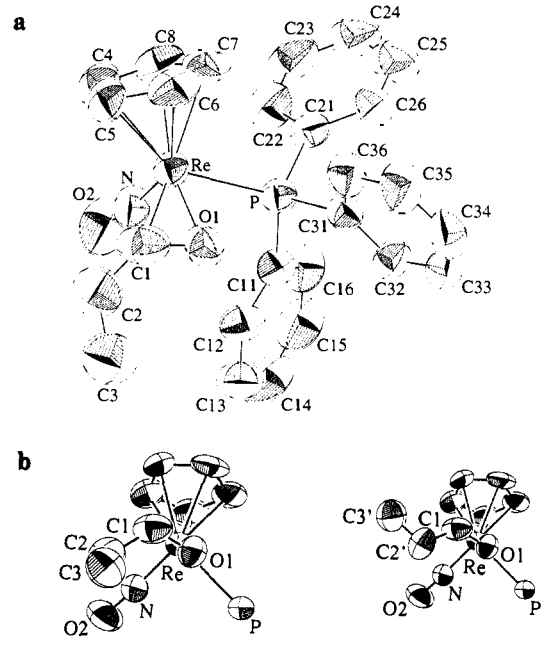

Figure 2. Structural views of the cation of propionaldehyde complex (*RS,SR*)-$[(\eta^5\text{-}C_5H_5)Re(NO)(PPh_3)(\eta^2\text{-}O{=}CHCH_2CH_3)]^+BF_4^-$ ((*RS,SR*)-$3b^+BF_4^-$): (a) numbering diagram for major C1–C2 rotamer; (b) Newman-type projections of major and minor rotamers with phenyl rings omitted.

Careful study of the IR ν_{NO} region of benzaldehyde complex (*RS,SR*)-$3e^+BF_4^-$ showed *two* bands (1739 and 1702 cm^{-1}; CH_2Cl_2, 26 °C) in a 84:16 area ratio (95:5 at −40 °C). The minor band was provisionally attributed to a σ isomer. Accordingly, an extensive series of substituted benzaldehyde complexes was prepared, as will be described elsewhere.[16] Depending upon the arene substitution pattern, temperature, and solvent, either π or σ binding modes can dominate. However, acetaldehyde and propionaldehyde complexes (*RS,SR*)-$3a,b^+X^-$ did not show any IR ν_{NO} absorbance in CH_2Cl_2 that could plausibly be attributed to a σ isomer (detection limit 3–4%), and isobutyraldehyde complex (*RS,SR*)-$3d^+BF_4^-$ exhibited only a weak shoulder suggestive of a small amount of a σ isomer. Unfortunately, the strong temperature dependence of these equilibria prevented an independent probe by standard low-temperature NMR decoalescence methodologies.[16]

3. Binding of Aldehyde Ligands: Conformation and Enantioface Selectivity. The Lewis acid fragment $[(\eta^5\text{-}C_5H_5)Re(NO)(PPh_3)]^+$ (I) has been shown to possess the high-lying d-orbital HOMO

(16) (a) Quirós Méndez, N.; Gladysz, J. A. Manuscript in preparation. (b) The thermochromism is due to π/σ equilibria. (c) Low-temperature ^{31}P NMR spectra of *p*-methoxybenzaldehyde complex $[(\eta^5\text{-}C_5H_5)Re(NO)(PPh_3)(O{=}CH(p\text{-}C_6H_4OCH_3))]^+BF_4^-$ show one σ and *two* π isomers (area ratios, $CDCl_2F$, −137 °C: ca. 28:58:14). Interestingly, the π isomer ratios increase significantly when the *p*-methoxy substituent is replaced by electron-withdrawing groups. The aliphatic aldehyde complexes show line broadening and other effects that suggest analogous dynamic equilibria, but with much smaller equilibrium concentrations of the alternative stereoisomers. These data will be reported in a subsequent paper.[16a]

(17) Merrifield, J. H.; Fernández, J. M.; Buhro, W. E.; Gladysz, J. A. *Inorg. Chem.* **1984**, *23*, 4022.

(18) (a) The first-order k_{obs} is consistent with either a dissociative or associative exchange mechanism: Espenson, J. H. *Chemical Kinetics and Reaction Mechanisms*; McGraw Hill: New York, 1981; pp 50–55. Experiments to distinguish these possibilities are planned. (b) In a separate experiment, (+)-Eu(hfc)$_3$ analysis showed the rhenium configuration to be largely retained under these exchange conditions (ca. 84% ee).

(19) Buhro, W. E.; Georgiou, S.; Fernández, J. M.; Patton, A. T.; Strouse, C. E.; Gladysz, J. A. *Organometallics* **1986**, *5*, 956.

(20) (a) Fernández, J. M.; Emerson, K.; Larsen, R. L.; Gladysz, J. A. *J. Chem. Soc., Chem. Commun.* **1988**, 37. (b) Dalton, D. M.; Gladysz, J. A. *J. Organomet. Chem.* **1989**, *370*, C17. (c) Dalton, D. M.; Fernández, J. M.; Emerson, K.; Larsen, R. L.; Arif, A. M.; Gladysz, J. A. Submitted for publication.

Table II. Summary of Crystallographic Data for Propionaldehyde Complex (*RS,SR*)-$[(\eta^5\text{-}C_5H_5)Re(NO)(PPh_3)(\eta^2\text{-}O{=}CHCH_2CH_3)]^+BF_4^-$ ((*RS,SR*)-**3b**$^+BF_4^-$) and Phenylacetaldehyde Complex (*RS,SR*)-$[\eta^5\text{-}C_5H_5)Re(NO)(PPh_3)(\eta^2\text{-}O{=}CHCH_2C_6H_5)]^+PF_6^-\cdot(CH_2Cl_2)_{0.5}$ ((*RS,SR*)-**3f**$^+PF_6^-\cdot(CH_2Cl_2)_{0.5}$)

	(*RS,SR*)-**3b**$^+BF_4^-$	(*RS,SR*)-**3f**$^+PF_6^-\cdot(CH_2Cl_2)_{0.5}$
mol formula	$C_{26}H_{26}BF_4NO_2PRe$	$C_{31}H_{28}F_6NO_2P_2Re\cdot(CH_2Cl_2)_{0.5}$
mol wt	688.5	851.2
cryst system	monoclinic	triclinic
space group	$P2_1/c$	$P\bar{1}$
cell dimensions (25 °C)		
a, Å	10.088 (2)	11.045 (3)
b, Å	17.762 (2)	13.315 (3)
c, Å	14.834 (2)	13.608 (4)
α, deg		117.20 (2)
β, deg	101.80 (1)	104.14 (2)
γ, deg		92.35 (2)
V, Å^3	2602 (1)	1698 (1)
Z	4	2
d_{calcd}, g/cm^3	1.73	1.66
cryst dimensions, mm	0.29 × 0.31 × 0.41	0.75 × 0.19 × 0.28
radiation, Å	λ(Mo Kα) 0.71069	λ(Mo Kα) 0.71069
data collection method	ω scans	Wyckoff ω
scan speed, deg/min	variable, 15–60	variable, 15–60
reflcns measured	$\pm h,+k,+l$	$\pm h,\pm k,+l$
scan range, deg	1.2	2
total bkdg time/scan time	0.2	1
no. of reflcns between std	97	97
totl unique data	7573	7704
obsd data, $I > 3\sigma(I)$	3256	4530
abs coeff (μ), cm^{-1}	50.6	40.2
no. of variables	331	465
$R = \sum(\|\|F_o\| - \|F_c\|\|)/\sum\|F_o\|$	0.0523	0.0542
$R_w = \sum(\|\|F_o\| - \|F_c\|\|)w^{1/2}/\sum\|F_o\|w^{1/2}$	0.0547	0.0562
goodness of fit	1.28	1.01
weighting factor, *w*	$K/(\sigma^2(F_o) + 0.0008(F_o)^2)$	$K/(\sigma^2(F_o) + 0.025(F_o)^2)$

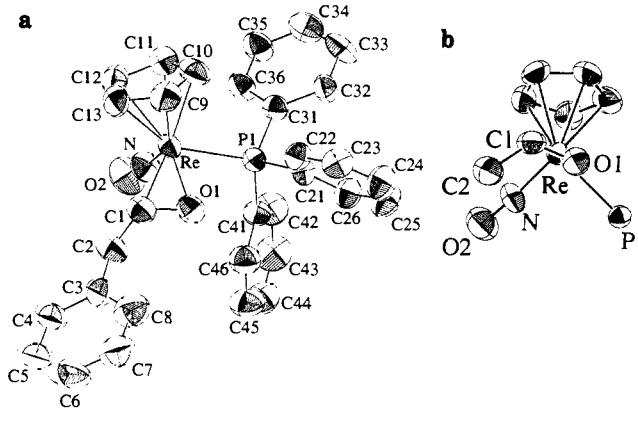

Figure 3. Structural views of the cation of phenylacetaldehyde complex (*RS,SR*)-$[(\eta^5\text{-}C_5H_5)Re(NO)(PPh_3)(\eta^2\text{-}O{=}CHCH_2C_6H_5)]^+PF_6^-\cdot(CH_2Cl_2)_{0.5}$ ((*RS,SR*)-**3f**$^+PF_6^-\cdot(CH_2Cl_2)_{0.5}$): (a) numbering diagram; (b) Newman-type projection with phenyl rings omitted.

depicted in Figure 1.[21] Accordingly, the formaldehyde ligand in **4**$^+PF_6^-$ adopts the solid-state conformation shown in II (Figure 1).[19] This is one of two orientations that maximize overlap of the vacant formaldehyde π^* acceptor orbital with the rhenium donor orbital. The alternative conformation in which the oxygen and carbon are interchanged is presumably disfavored due to CH_2/PPh_3 steric interactions. This conformation should be even less accessible with substituted aldehydes. Thus, we anticipated two possible structures, III (*RS,SR*) and IV (*RR,SS*),[15b] for substituted aldehyde complexes of Lewis acid I (Figure 1). These are diastereomeric and differ in the aldehyde enantioface bound to the rhenium. In the former, the aldehyde substituent is directed at the small NO ligand, in a syn or endo relationship. In the latter, the substituent is directed at (or is syn or endo to) the medium-sized cyclopentadienyl ligand. Hence, we expected III to be considerably more stable than IV.

Solid-state structures were probed first. X-ray data were acquired on crystals of (*RS,SR*)-**3b**$^+BF_4^-$ and (*RS,SR*)-**3f**$^+PF_6^-\cdot(CH_2Cl_2)_{0.5}$ as summarized in Table II. Refinement, described in the Experimental Section, yielded the structures shown in Figures 2 and 3. The propionaldehyde ligand in (*RS,SR*)-**3b**$^+BF_4^-$ was disordered about the C1–C2 bond, giving a 61:39 mixture of conformers. Only the major conformer is shown in Figure 2a, whereas both are given in Figure 2b. In all cases, the aldehyde ligand conformation and enantioface bound to the rhenium corresponds to that shown in III (Figure 1). Bond lengths and angles are summarized in Tables III and IV, and atomic coordinates and

Table III. Key Bond Lengths (Å) and Angles (deg) in (*RS,SR*)-**3b**$^+BF_4^-$[a]

Re–O(1)	2.054 (8)	Re–C(8)	2.261 (12)
Re–C(1)	2.191 (11)	C(1)–C(2)	1.510 (14)
O(1)–C(1)	1.256 (14)	C(1)–C(2′)	1.510 (16)
Re–P	2.442 (3)	C(2)–C(3)	1.540 (15)
Re–N	1.754 (10)	C(2′)–C(3′)	1.540 (37)
N–O(2)	1.178 (15)	C(4)–C(5)	1.432 (19)
Re–C(4)	2.262 (13)	C(4)–C(8)	1.387 (18)
Re–C(5)	2.317 (11)	C(5)–C(6)	1.416 (18)
Re–C(6)	2.345 (12)	C(6)–C(7)	1.362 (17)
Re–C(7)	2.313 (12)	C(7)–C(8)	1.471 (20)
N–Re–P	89.9 (3)	Re–C(1)–C(2′)	127.1 (12)
Re–N–O(2)	172.9 (10)	O(1)–C(1)–C(2′)	123.7 (13)
N–Re–O(1)	104.5 (4)	C(1)–C(2)–C(3)	104.6 (9)
N–Re–C(1)	95.1 (4)	C(1)–C(2′)–C(3′)	104.6 (13)
P–Re–O(1)	77.7 (2)	C(5)–C(4)–C(8)	109.2 (12)
P–Re–C(1)	110.7 (3)	C(4)–C(5)–C(6)	106.8 (10)
Re–O(1)–C(1)	78.8 (7)	C(5)–C(6)–C(7)	109.5 (12)
Re–C(1)–O(1)	66.9 (6)	C(6)–C(7)–C(8)	108.3 (12)
Re–C(1)–C(2)	108.1 (8)	C(4)–C(8)–C(7)	106.2 (11)
O(1)–C(1)–C(2)	118.9 (13)		

[a] Primed atoms are for the minor propionaldehyde ligand conformation. Bond lengths and angles involving the PPh_3 ligand have been omitted.

Table IV. Key Bond Lengths (Å) and Angles (deg) in (*RS,SR*)-**3f**$^+PF_6^-\cdot(CH_2Cl_2)_{0.5}$

Re–O(1)	2.062 (9)	C(2)–C(3)	1.491 (19)
Re–C(1)	2.155 (12)	C(3)–C(4)	1.431 (13)
O(1)–C(1)	1.318 (11)	C(3)–C(8)	1.400 (18)
Re–P(1)	2.437 (3)	C(4)–C(5)	1.364 (22)
Re–N	1.766 (9)	C(5)–C(6)	1.433 (23)
N–O(2)	1.135 (12)	C(6)–C(7)	1.417 (16)
Re–C(9)	2.328 (14)	C(7)–C(8)	1.406 (23)
Re–C(10)	2.313 (13)	C(9)–C(10)	1.391 (17)
Re–C(11)	2.267 (15)	C(9)–C(13)	1.424 (14)
Re–C(12)	2.272 (15)	C(10)–C(11)	1.400 (16)
Re–C(13)	2.303 (14)	C(11)–C(12)	1.396 (13)
C(1)–C(2)	1.498 (15)	C(12)–C(13)	1.400 (19)
N–Re–P(1)	88.7 (3)	C(2)–C(3)–C(8)	123.4 (9)
Re–N–O(2)	173.1 (12)	C(4)–C(3)–C(8)	119.1 (13)
O(1)–Re–C(1)	36.3 (3)	C(3)–C(4)–C(5)	122.3 (13)
N–Re–O(1)	106.0 (4)	C(4)–C(5)–C(6)	118.5 (11)
N–Re–C(1)	92.3 (4)	C(5)–C(6)–C(7)	120.3 (15)
P(1)–Re–O(1)	78.8 (2)	C(6)–C(7)–C(8)	119.9 (14)
P(1)–Re–C(1)	112.2 (3)	C(3)–C(8)–C(7)	120.0 (10)
Re–O(1)–C(1)	75.7 (7)	C(10)–C(9)–C(13)	106.5 (11)
Re–C(1)–O(1)	68.0 (6)	C(9)–C(10)–C(11)	107.8 (9)
Re–C(1)–C(2)	120.0 (8)	C(10)–C(11)–C(12)	110.4 (11)
O(1)–C(1)–C(2)	122.0 (12)	C(11)–C(12)–C(13)	105.4 (9)
C(1)–C(2)–C(3)	111.2 (10)	C(9)–C(13)–C(12)	109.9 (10)
C(2)–C(3)–C(4)	117.6 (11)		

(21) (a) Kiel, W. A.; Lin, G.-Y.; Constable, A. G.; McCormick, F. B.; Strouse, C. E.; Eisenstein, O.; Gladysz, J. A. *J. Am. Chem. Soc.* **1982**, *104*, 4865. (b) Georgiou, S.; Gladysz, J. A. *Tetrahedron* **1986**, *42*, 1109. (c) Schilling, B. E. R.; Hoffmann, R.; Faller, J. *J. Am. Chem. Soc.* **1979**, *101*, 592.

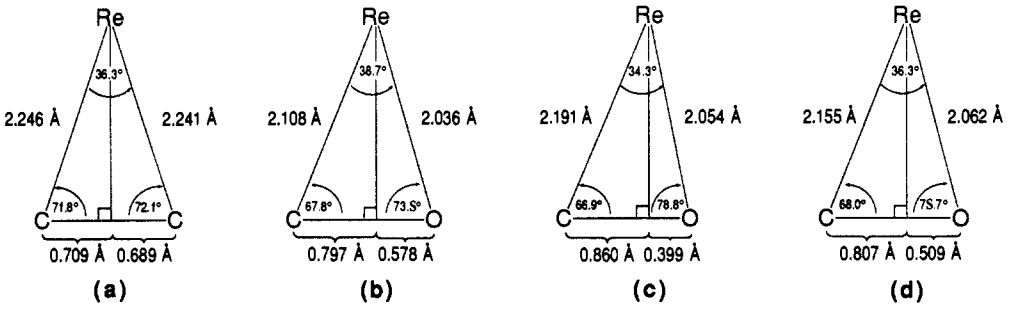

Figure 4. Comparison of π ligand slippage in (a) alkene complex (*RR,SS*)-$[(\eta^5\text{-}C_5H_5)Re(NO)(PPh_3)(H_2C{=}CHCH_2C_6H_5)]^+PF_6^-$, (b) formaldehyde complex $\mathbf{4}^+PF_6^-$, (c) (*RS,SR*)-$\mathbf{3b}^+BF_4^-$, and (d) (*RS,SR*)-$\mathbf{3f}^+PF_6^-\cdot(CH_2Cl_2)_{0.5}$.

anisotropic thermal parameters are given in the supplementary material.

Structural features of the Re–C1–O1 planes in (*RS,SR*)-$\mathbf{3b}^+BF_4^-$ and (*RS,SR*)-$\mathbf{3f}^+PF_6^-\cdot(CH_2Cl_2)_{0.5}$ were examined. First, these planes made 15.5° and 22.8° angles, respectively, with the Re–PPh_3 bonds. The corresponding angles with the Re–NO bonds were 71.0° and 65.6°. These are close to the 0° and 90° angles shown in idealized structure III. As a check, the angles of the Re–C1–O1 planes and the planes defined by the Re–PPh_3 bonds and C1–O1 midpoints were calculated. The values (15.6°, 22.9°) closely matched those obtained above. Finally, the Re–C1–O1 moieties were distorted or "slipped", with the rhenium significantly closer to oxygen than carbon. These features are illustrated in Figure 4.

In each complex, the C1–C2 bonds were bent out of the π nodal planes of the free aldehydes. In order to quantify this feature, which slightly attenuates rhenium fragment/aldehyde ligand steric interactions, planes were defined that contained C1 and O1 but were perpendicular to the Re–C1–O1 planes. The angles of the C1–C2 bonds with these planes were 24.8° and 7.5° in the two conformations of (*RS,SR*)-$\mathbf{3b}^+BF_4^-$ and 19.0° in (*RS,SR*)-$\mathbf{3f}^+PF_6^-$. In the corresponding free aldehydes, these angles would be 0°.

Complexes (*RS,SR*)-$\mathbf{3a\text{–}f}^+X^-$ also *appeared* diastereomerically pure in solution by the spectroscopic criteria in Table I. However, reaction of $\mathbf{2}^+BF_4^-$ and monosubstituted alkenes (which are approximately isosteric to aldehydes) gives complexes $[(\eta^5\text{-}C_5H_5)Re(NO)(PPh_3)(H_2C{=}CHR)]^+BF_4^-$ that are ca. 2:1 *mixtures* of diastereomers (analogous to III and IV).[22] These can be independently prepared, are easily distinguished by NMR, and equilibrate at 90–100 °C to ca. 95:5 mixtures of diastereomers. Thus, we were concerned that (*SR,RS*)-$\mathbf{3a\text{–}f}^+X^-$ might similarly exist as mixtures of diastereomers in solution. Low-temperature NMR spectra were acquired to probe for this possibility. However, no signal decoalescence was noted for any of the aliphatic aldehyde complexes.[16c]

Additional probes of the solution structures of (*RS,SR*)-$\mathbf{3a\text{–}f}^+X^-$ were sought. Hence, difference NOE ^1H NMR experiments[23] were conducted in CD_2Cl_2 as previously described.[9c] First, the cyclopentadienyl protons of formaldehyde complex $\mathbf{4}^+PF_6^-$ were irradiated. A 2.2% enhancement was observed in one aldehydic proton (δ 4.75), but none in the other (δ 4.30). Thus, the δ 4.75 proton was assigned as the one nearer to the cyclopentadienyl ligand in II (Figure 1).

Identical NOE experiments were conducted with (*RS,SR*)-$\mathbf{3a\text{–}f}^+PF_6^-$. Aldehyde proton enhancements were 7.0%, 5.5%, 7.1%, 4.9%, 3.4%, and 4.0%, respectively. Hence, it was concluded that the dominant aldehyde ligand conformations in solution have (1) the aldehyde carbon anti to the PPh_3 ligand and (2) the aldehyde proton syn to the cyclopentadienyl ligand as in III.

Scheme II. Syntheses of Alkoxide Complexes $(\eta^5\text{-}C_5H_5)Re(NO)(PPh_3)(OCH_2R)$ (**6**)

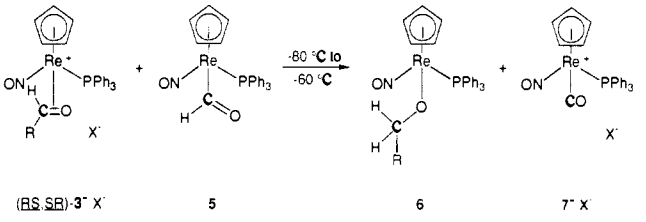

4. Reduction of Aldehyde Complexes to Alkoxide Complexes. Formyl complexes, L_nMCHO, have frequently been employed as hydride donors.[24] Further, the chiral, racemic formyl complex $(\eta^5\text{-}C_5H_5)Re(NO)(PPh_3)(CHO)$ (**5**)[13] has previously been shown to reduce formaldehyde complex $\mathbf{4}^+PF_6^-$, giving methoxide complex $(\eta^5\text{-}C_5H_5)Re(NO)(PPh_3)(OCH_3)$ and carbonyl complex $[(\eta^5\text{-}C_5H_5)Re(NO)(PPh_3)(CO)]^+PF_6^-$ ($\mathbf{7}^+PF_6^-$).[19] Thus, aldehyde complexes (*RS,SR*)-$\mathbf{3a\text{–}f}^+X^-$ and **5** were similarly reacted in CH_2Cl_2 at −80 °C. Workup gave alkoxide complexes $(\eta^5\text{-}C_5H_5)Re(NO)(PPh_3)(OCH_2R)$ (**6**) in 95–80% yields (Scheme II). Separate NMR experiments showed the reaction to be spectroscopically quantitative and proceed over the temperature range of −80 to −60 °C. When desired, the carbonyl complex byproduct $\mathbf{7}^+X^-$ could also be isolated in 95–85% yields.

Alkoxide complexes **6a–f** were isolated as analytically pure, orange-red solids that were stable to air for brief periods of time. Crystals could be obtained from toluene/hexane. Solutions of **6a–f** were very sensitive toward air and electrophiles, which resulted in yield loss when workups were not carefully conducted. Complexes **6a–f** were characterized analogously to (*RS,SR*)-$\mathbf{3a\text{–}f}^+X^-$, as summarized in Table V and the Experimental Section. Spectroscopic properties resembled those of the methoxide complex reported earlier.[19] The ^1H NMR resonances of the diastereotopic $-OCH_2$ methylene hydrogens were in all cases well-separated, as shown in Figure 5. This feature is relevant to stereoselectivity assays utilized below.

Formyl complex **5** did not reduce dichloromethane solutions of free aldehydes over the course of 24 h at 25 °C. Hence, aldehydes are dramatically activated by Lewis acid I toward nucleophilic attack. Reactions of (*RS,SR*)-$\mathbf{3a\text{–}f}^+X^-$ with conventional boron and aluminum hydride reagents (e.g., $Li(C_2H_5)_3BH$) did afford spectroscopically detectable quantities of alkoxide complexes **6**. However, numerous byproducts also formed, possibly due to reaction of the alkoxide complexes with the Lewis acids also generated (vide infra). Note that formyl complex **5** gives an easily precipitated, nonacidic product ($\mathbf{7}^+X^-$) following hydride transfer (Scheme II).

Optically active aldehyde complexes (+)-(*RS*)-$\mathbf{3a\text{–}f}^+BF_4^-$ and **5** reacted similarly to give optically active alkoxide complexes (+)-(*R*)-**6a–f**. These were considerably more soluble than the racemates and could not be crystallized as readily. Their spectroscopic properties were identical with those of the racemates, and they were further characterized by optical rotations (Experimental Section).[15] The stereochemistry at rhenium (retention)

(22) (a) Bodner, G. S.; Fernández, J. M.; Arif, A. M.; Gladysz, J. A. *J. Am. Chem. Soc.* **1988**, *110*, 4082. (b) Bodner, G. S.; Peng, T.-S.; Arif, A. M.; Gladysz, J. A. *Organometallics* **1990**, *9*, 1191. (c) Kiel, W. A.; Lin, G.-Y.; Bodner, G. S.; Gladysz, J. A. *J. Am. Chem. Soc.* **1983**, *105*, 4958.

(23) Sanders, J. K. M.; Hunter, B. K. *Modern NMR Spectroscopy*; Oxford University Press: New York, 1987; Chapter 6.

(24) Gladysz, J. A. *Adv. Organomet. Chem.* **1982**, *23*, 1.

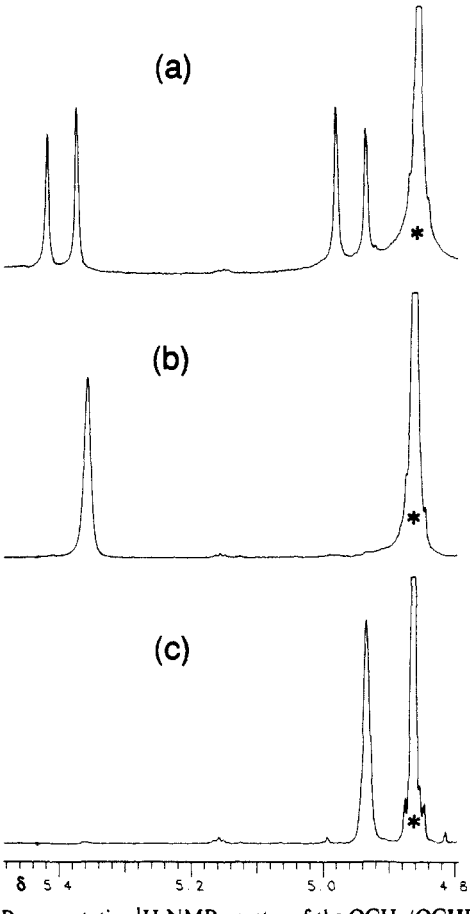

Figure 5. Representative ^1H NMR spectra of the $OCH_2/OCHD$ protons of alkoxide complexes **6**-d_x: (a) $(\eta^5\text{-}C_5H_5)Re(NO)(PPh_3)(OCH_2C_6H_5)$ (**6e**); (b) (+)-(*RR*)-**6e**-d_1 (entry 16, Scheme IV); (c) (+)-(*RS*)-**6e**-d_1 (entry 18, Scheme IV). The cyclopentadienyl ligand resonances are designated by asterisks.

was assigned by analogy to that observed for a variety of reactions involving nucleophilic attack upon coordinated ligands.[7a-d,9a,b] This assignment was supported by the signs of the $[\alpha]^{25}_{589}$ (vide supra).[15]

5. Reactions of Alkoxide Complexes. We sought to develop reactions that would cleanly detach the alkoxide ligands in **6a–f**. We further sought reactions that would facilitate stereochemical analyses, both at rhenium in the optically active compounds synthesized above and at carbon in the aldehyde reduction products described below.

First, optically active benzoxide complex (+)-(*R*)-**6e** was treated with HI at −80 °C (2 equiv, CH_2Cl_2; Scheme III, eq 1). The sample was warmed to −45 °C, and GC analysis showed the formation of benzyl alcohol (92%). Chiral HPLC analysis showed the formation of previously characterized iodide complex (+)-(*R*)-$(\eta^5\text{-}C_5H_5)Re(NO)(PPh_3)(I)$ ((+)-(*R*)-**8**)[17] in >99% ee. Workup gave (+)-(*R*)-**8** in 99% yield and an ee of 84% ([α]) to 87% (HPLC). The formation of benzyl alcohol was quantitative by ^1H NMR, as assayed in a similar reaction conducted in CD_2Cl_2. Complex **8** exhibits good configurational stability in solution[17] but is slowly racemized by some component of the reaction mixture.

Benzoxide complex (+)-(*R*)-**6e** was also treated with $(CH_3)_3SiI$ (1.0 equiv, C_6D_6, 20 °C; Scheme III, eq 2). A ^1H NMR spectrum showed the clean formation of benzyl trimethylsilyl ether (80%) and (+)-(*R*)-**8** (90%). The identity of the former was verified by GC (78%), and the latter was isolated in 89% yield and 86 ± 2% ee. In experiments conducted with excess $(CH_3)_3SiI$, varying amounts of benzyl iodide also formed.

A preliminary reaction was conducted with racemic **6e** and acetyl iodide (2.0 equiv, CD_2Cl_2, 0 °C). A ^1H NMR spectrum showed the clean formation of benzyl acetate and **8**. GC analysis verified the presence of benzyl acetate (89%), and workup gave **8** in 60% yield.

Scheme III. Rhenium–Oxygen Bond Cleavage Reactions of Optically Active Alkoxide Complexes

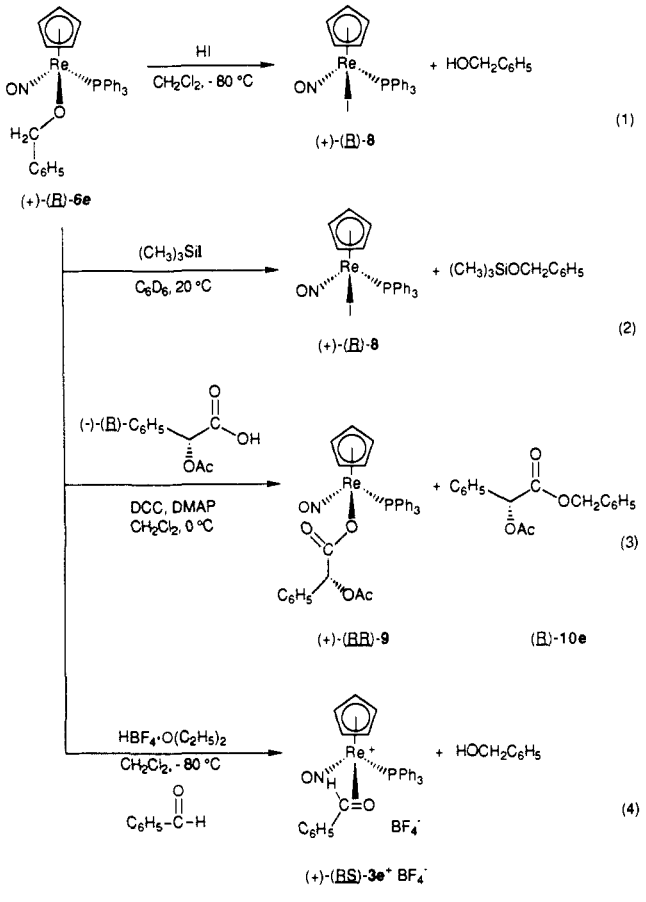

Another route from alkoxide complexes to esters was studied in preparation for analyses of reactions described below. Complex (+)-(*R*)-**6e** was treated (CH_2Cl_2, 0 °C) with (−)-(*R*)-*O*-acetylmandelic acid ((−)-(*R*)-$C_6H_5CH(OAc)COOH$; 2.5 equiv, 99.5% ee), 4-(dimethylamino)pyridine (DMAP, 0.15 equiv), and dicyclohexylcarbodiimide (DCC, 3.0 equiv). Workup gave *O*-acetylmandelate complex (+)-(*RR*)-$(\eta^5\text{-}C_5H_5)Re(NO)(PPh_3)(O(C{=}O)CH(OAc)C_6H_5)$ ((+)-(*RR*)-**9**) in 97% yield and >99% de and ester (*R*)-$C_6H_5CH(OAc)COOCH_2C_6H_5$ ((*R*)-**10e**) in >99% yield (Scheme III, eq 3).[25,26] An authentic sample of the opposite *O*-acetylmandelate complex diastereomer, (+)-(*RS*)-**9**, was similarly synthesized from (+)-(*R*)-**6e** and (+)-(*S*)-*O*-acetylmandelic acid. These complexes were characterized analogously to **6a–f**, and were easily distinguished by ^1H, $^{13}C\{^1H\}$, and $^{31}P\{^1H\}$ NMR (Experimental Section). The reagents DMAP/DCC have frequently been utilized to prepare esters from *O*-acetylmandelic acid and alcohols, and benzyl alcohol is likely the initial organic product under our reaction conditions.[25]

We sought to recycle the rhenium moiety from one of the preceding types of reactions to an optically active aldehyde complex. Accordingly, (+)-(*R*)-**6e** was treated with $HBF_4{\cdot}O(C_2H_5)_2$ (1.2 equiv, CH_2Cl_2, −80 °C; Scheme III, eq 4). Benzaldehyde (5.0 equiv) was then added. Workup gave benzaldehyde complex (+)-(*RS*)-**3e**$^+BF_4^-$ (82%) of 99 ± 1% ee, and the formation of benzyl alcohol (72%) was verified by GC.

6. Deuteride Reduction of Aldehyde Complexes. We sought to determine whether aldehyde complexes $\mathbf{3}^+X^-$ would undergo

(25) (a) Hassner, A.; Alexanian, V. *Tetrahedron Lett.* **1978**, *19*, 4475. (b) Parker, D. *J. Chem. Soc., Perkin Trans. II* **1983**, 83. (c) Whitesell, J. K.; Reynolds, D. *J. Org. Chem.* **1983**, *48*, 3548. (d) Ramalingam, K.; Nanjappan, P.; Kalvin, D. M.; Woodard, R. W. *Tetrahedron* **1988**, *44*, 5597.

(26) Although [α] for *O*-acetylmandelate esters **10a–f**-d_n were not measured, esters of (−)-(*R*)-*O*-acetylmandelic acid and simple aliphatic alcohols are levorotatory: Bevinakatti, H. S.; Banerji, A. A.; Newadkar, R. V. *J. Org. Chem.* **1989**, *54*, 2453.

Table V. Spectroscopic Characterization of Alkoxide Complexes (η^5-C_5H_5)Re(NO)(PPh_3)(OCH_2R) (6)

complex (R)	IR ν_{NO},[a] cm^{-1}	^1H NMR,[b] δ	$^{13}C\{^1H\}$ NMR,[c] ppm	$^{31}P\{^1H\}$ NMR,[d] ppm
6a (CH_3)	1607 (vs)	7.79–7.69 (m, 6 H of 3 C_6H_5), 7.13–6.97 (m, 9 H of 3 C_6H_5), 4.88 (s, C_5H_5), 4.24 (m, CHH'), 4.00 (m, CHH'), 1.27 (t, J = 6.9, CH_3)	PPh_3 at 136.1 (d, J = 51.3, *i*), 134.9 (d, J = 10.8, *o*), 130.6 (s, *p*);[e] 90.9 (s, C_5H_5), 81.7 (d, J = 5.6, CH_2), 21.6 (s, CH_3)	17.2 (s)
6b (CH_2CH_3)	1607 (vs)	7.75–7.68 (m, 6 H of 3 C_6H_5), 7.07–6.99 (m, 9 H of 3 C_6H_5), 4.87 (s, C_5H_5), 4.08 (dt, J = 9.8, 6.0, OCHH'), 3.96 (dt, J = 9.9, 6.6, OCHH'), 1.61 (m, CCH_2C), 0.93 (t, J = 7.5, CH_3)	PPh_3 at 135.6 (d, J = 50.8, *i*), 134.4 (d, J = 10.2, *o*), 130.1 (d, J = 2.5, *p*), 128.4 (d, J = 10.8, *m*); 90.6 (d, J = 2.6, C_5H_5), 88.9 (dd, J = 6.2, OCH_2), 29.5 (CCH_2C), CCH_2C), 11.4 (s, CH_3)	17.2 (s)
6c ($CH_2CH_2CH_3$)	1607 (vs)	7.75–7.68 (m, 6 H of 3 C_6H_5), 7.08–7.00 (m, 9 H of 3 C_6H_5), 4.87 (s, C_5H_5), 4.13 (dt, J = 10.0, 6.4, OCHH'), 4.00 (dt, J = 10.0, 6.4, OCHH'), 1.61 (m, CH_2), 1.36 (m, CH_2), 0.97 (t, J = 7.3, CH_3)	PPh_3 at 135.7 (d, J = 50.6, *i*), 134.4 (d, J = 10.5, *o*), 130.3 (d, J = 2.1, *p*), 128.4 (d, J = 10.0, *m*); 90.6 (d, J = 2.0, C_5H_5), 86.6 (d, J = 6.4, OCH_2), 38.5 (s, $OCCH_2$), 14.8 (s, CH_3)	17.1 (s)
6d ($CH(CH_3)_2$)	1607 (vs)	7.74–7.67 (m, 6 H of 3 C_6H_5), 7.07–6.99 (m, 9 H of 3 C_6H_5), 4.87 (s, C_5H_5), 4.06 (dd, J = 9.6, 5.5, OCHH'), 3.62 (dd, J = 9.6, 6.4, OCHH'), 1.72 (m, CH), 0.90 (d, J = 6.6, CH_3), 0.89 (d, J = 6.7, CH_3')	PPh_3 at 136.9 (d, J = 50.9, *i*), 134.4 (d, J = 10.3, *o*), 130.2 (d, J = 2.5, *p*), 128.4 (d, J = 10.9, *m*); 94.9 (d, J = 6.3, OCH), 90.7 (d, J = 1.4, C_5H_5), 34.4 (s, CH), 20.2 (s, CH_3), 20.0 (s, C'H_3)	17.3 (s)
6e (C_6H_5)	1610 (vs)	7.74–6.97 (m, 4 C_6H_5), 5.40 (d, J = 13.6, CHH'), 4.96 (d, J = 13.6, CHH'), 4.86 (s, C_5H_5)	PPh_3 at 135.6 (d, J = 50.6, *i*), 134.4 (d, J = 10.2, *o*), 130.2 (d, J = 1.4, *p*), 128.5 (d, J = 10.5, *m*); CPh at 147.8 (s, *i*), 128.0 (s), 126.5 (s);[e] 90.5 (d, J = 2.6, C_5H_5), 89.2 (d, J = 6.2 CH_2)	18.0 (s)
6f ($CH_2C_6H_5$)	1622 (vs)	7.73–6.99 (m, 4 C_6H_5), 4.76 (s, C_5H_5), 4.36 (ddd, J = 9.9, 6.9, 4.8, OCHH'), 4.12 (ddd, J = 9.9, 8.2, 7.3, OCHH'), 2.75 (m, $CH_2C_6H_5$)	PPh_3 at 136.0 (d, J = 51.2, *i*), 134.8 (d, J = 10.8, *o*), 130.6 (s, *p*), 128.7 (d, J = 9.3, *m*); CPh at 142.6 (s, *i*), 130.0 (s), 125.8 (s);[e] 90.9 (s, C_5H_5), 88.9 (d, J = 5.7, OCH_2), 43.3 (s, $CH_2C_6H_5$)	17.6 (s)

[a] KBr disk. [b] Recorded at 300 MHz in C_6D_6 at ambient probe temperature and referenced to internal $Si(CH_3)_4$. All couplings are in Hz. [c] Recorded at 75 MHz in C_6D_6 at ambient probe temperature and referenced to C_6D_6 (128.0 ppm). All couplings are in Hz and are to ^{31}P unless noted. Assignments of phenyl carbon resonances were made as described in footnote *c* of Table I in ref 19. [d] Recorded at 121 MHz (unlocked) in C_6D_6 at ambient probe temperature and referenced to external 85% H_3PO_4. [e] One phenyl resonance obscured by C_6D_6.

stereoselective nucleophilic additions. In view of the high-yield hydride additions described above, initial efforts were directed at analogous deuteride additions. Hence, *racemic* aldehyde complexes (*RS,SR*)-**3a–f**$^+BF_4^-$ were treated with *racemic* deuterioformyl complex (η^5-C_5H_5)Re(NO)(PPh_3)(CDO) (**5**-d_1, 1.0 equiv, >99% labeled) in CH_2Cl_2 at −80 °C. Workup as above gave deuterated alkoxide complexes (η^5-C_5H_5)Re(NO)(PPh_3)(OCHDR) (**6a–f**-d_1) as 97–92:3–8 mixtures of (*RR,SS*)/(*RS,SR*) diastereomers (Scheme IV; entries 1–6), as assayed by the relative areas of the −OCHD ^1H NMR resonances (see Figure 5).[27] Interestingly, the downfield $-OCH_2$ ^1H NMR resonance of **6a** was absent in (*RS,SR*)-**6a**-d_1, whereas the upfield resonances of **6b–f** were absent in (*RS,SR*)-**6b–f**-d_1. The configurations at carbon were assigned as described below.

We sought to repeat these highly stereoselective reductions with *optically active* aldehyde complexes (+)-(*RS*)-**3a–f**$^+BF_4^-$. This would afford optically active deuterioalkoxide complexes, which could be transformed by the types of cleavage reactions developed in Scheme III to optically active organic products of known carbon absolute configurations. This would establish the stereochemistry of the alkoxide complexes and the *net* direction of deuteride addition.

We initially envisioned conducting a series of experiments with (+)-(*RS*)-**3a–f**$^+BF_4^-$ and *racemic* deuterioformyl complex **5**-d_1 (e.g., Scheme IV, entry 7). However, preliminary observations hinted that the enantiomers of **5**-d_1 gave different reduction stereoselectivities. Hence, we conducted one series of reductions with (+)-(*S*)-**5**-d_1 (Scheme IV, entries 8–17) and another with (−)-(*R*)-**5**-d_1 (Scheme IV, entries 19–26). These gave optically active deuterioalkoxide complexes (+)-**6a–f**-d_1 as 99–94:1–6 and 91–84:9–16 mixtures of (*RR*)/(*RS*) diastereomers, respectively.[27] Hence, the deuterioalkoxide complex diastereomer ratios were highest with (+)-(*S*)-**5**-d_1, intermediate with racemic **5**-d_1, and lowest with (−)-(*R*)-**5**-d_1. Similar phenomena have previously been observed in reactions involving two chiral, optically active species. The more stereoselective reaction is commonly referred to as affording "double asymmetric induction".[28] This effect was not discerned in previous experiments cited in our preliminary communication.[12]

As a check on the preceding data, optically active *deuterio*benzaldehyde complex (+)-(*RS*)-**3e**$^+$-d_1-BF_4^- was treated with optically active *protio*formyl complex (+)-(*S*)-**5** (Scheme IV, entry 18). As expected, the deuterioalkoxide complex formed, (+)-(*RS*)-**6**-d_1, was diastereomeric to that obtained above (entries 14–16). A ^1H NMR spectrum is shown in Figure 5.

Finally, the time scales of the preceding reactions were probed. Equimolar amounts of optically active benzaldehyde complex (+)-(*RS*)-**3e**$^+BF_4^-$ and optically active deuterioformyl complex (−)-(*R*)-**5**-d_1 were frozen in CD_2Cl_2. Samples (0.30 M) were placed in −95.4 and −80.0 °C NMR probes, and rates were measured by the disappearance and appearance of cyclopentadienyl resonances. Second-order treatment gave k_{obs} of approximately 6.2×10^{-3} M^{-1} s^{-1} ($t_{1/2}$ = 1.5 h) and 6.7×10^{-2} M^{-1} s^{-1} ($t_{1/2}$ = 7.7 min). The corresponding reactions of (+)-(*RS*)-**3e**$^+BF_4^-$ and enantiomeric formyl complex (+)-(*S*)-**5**-d_1 were too rapid to measure. In principle, quantitative rate comparisons

(27) (a) Since the diastereomers of **6a–f**-d_1 differ only by isotopic substitution, their ratios should not change significantly upon workup. Nonetheless, these compounds were not purified as rigorously as undeuterated **6a–f** prior to analysis (Experimental Section). Also, reactions were conducted in the presence of small amounts of deuteriomethyl complex **1**-d_3, an impurity that is removed from deuterioformyl complex **5**-d_1 only with substantial yield loss. (b) We consider the numerical components of the diastereomer ratios in Scheme IV accurate to ±2—i.e., 92.0:8.0 ≡ (92.0 ± 2):(8.0 ± 2). These are expressed to the nearest half-integer to facilitate conversion to percent de.

(28) Masamune, S.; Choy, W.; Peterson, J. S.; Sita, L. R. *Angew. Chem., Int. Ed. Engl.* **1985**, *24*, 1.

Scheme IV. Deuteride Reduction of Aldehyde Complexes

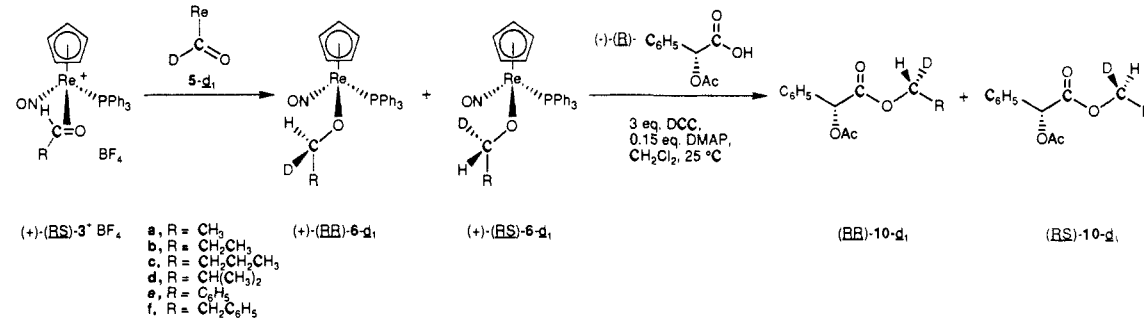

entry	aldehyde complex	formyl reductant	ratio (±)-(*RR*,*SS*)-**6**-d_1/(±)-(*RS*,*SR*)-**6**-d_1 or (+)-(*RR*)-**6**-d_1/(+)-(*RS*)-**6**-d_1	yield (%)[a]	ratio (*RR*)-**10**-d_1/(*RS*)-**10**-d_1	yield (%)[a]
1	(±)-(*RS*,*SR*)-**3a**$^+BF_4^-$	(±)-**5**-d_1	93.0:7.0 (86% de)	82	50:50	90
2	(±)-(*RS*,*SR*)-**3b**$^+BF_4^-$	(±)-**5**-d_1	95.0:5.0 (90% de)	86	50:50	83
3	(±)-(*RS*,*SR*)-**3c**$^+BF_4^-$	(±)-**5**-d_1	96.5:3.5 (93% de)	94	50:50	62
4	(±)-(*RS*,*SR*)-**3d**$^+BF_4^-$	(±)-**5**-d_1	94.5:5.5 (89% de)	95	50:50	94
5	(±)-(*RS*,*SR*)-**3e**$^+BF_4^-$	(±)-**5**-d_1	95.5:4.5 (91% de)	99	50:50	89
6	(±)-(*RS*,*SR*)-**3f**$^+BF_4^-$	(±)-**5**-d_1	92.5:7.5 (85% de)	98	50:50	87
7	(+)-(*RS*)-**3e**$^+BF_4^-$	(±)-**5**-d_1	92.5:7.5 (85% de)	95		
8	(+)-(*RS*)-**3a**$^+BF_4^-$	(+)-(*S*)-**5**-d_1	95.0:5.0 (90% de)	88	96.0:4.0 (92% de)	90
9		(+)-(*S*)-**5**-d_1	95.5:4.5 (91% de)	91		
10		(+)-(*S*)-**5**-d_1	96.5:3.5 (93% de)	82		
11	(+)-(*RS*)-**3b**$^+BF_4^-$	(+)-(*S*)-**5**-d_1	95.5:4.5 (91% de)	91	98.0:2.0 (96% de)	98
12	(+)-(*RS*)-**3c**$^+BF_4^-$	(+)-(*S*)-**5**-d_1	94.5:5.5 (89% de)	68	95.5:4.5 (91% de)	86
13	(+)-(*RS*)-**3d**$^+BF_4^-$	(+)-(*S*)-**5**-d_1	98.5:1.5 (97% de)	86	98.0:2.0 (96% de)[b]	91
14	(+)-(*RS*)-**3e**$^+BF_4^-$	(+)-(*S*)-**5**-d_1	99.0:1.0 (98% de)	>99	99.0:1.0 (98% de)	89
15			99.0:1.0 (98% de)	97	99.0:1.0 (98% de)	97
16			≥99.0:1.0 (≥98% de)	96		
17	(+)-(*RS*)-**3f**$^+BF_4^-$	(+)-(*S*)-**5**-d_1	96.0:4.0 (92% de)	87	94.0:6.0 (88% de)[b]	98
18	(+)-(*RS*)-**3e**$^+$-d_1-BF_4^-	(+)-(*S*)-**5**	1.0:99.0 (98% de)	>99		
19	(+)-(*RS*)-**3a**$^+BF_4^-$	(−)-(*R*)-**5**-d_1	89.5:10.5 (79% de)	89	91.0:9.0 (82% de)	78
20			91.0:9.0 (82% de)	88		
21	(+)-(*RS*)-**3b**$^+BF_4^-$	(−)-(*R*)-**5**-d_1	85.5:14.5 (71% de)	85		
22	(+)-(*RS*)-**3c**$^+BF_4^-$	(−)-(*R*)-**5**-d_1	87.5:12.5 (75% de)	70		
23	(+)-(*RS*)-**3d**$^+BF_4^-$	(−)-(*R*)-**5**-d_1	85.5:14.5 (71% de)	83		
24	(+)-(*RS*)-**3e**$^+BF_4^-$	(−)-(*R*)-**5**-d_1	88.0:12.0 (76% de)	98	87.0:13.0 (74% de)	84
25			85.0:15.0 (70% de)	97		
26	(+)-(*RS*)-**3f**$^+BF_4^-$	(−)-(*R*)-**5**-d_1	84.0:16.0 (68% de)	87		

[a] All yields are for isolated products; see text. [b] Assayed by 500-MHz ^1H NMR with decoupling; see text.

might be possible at lower temperatures. However, CD_2Cl_2 freezes near −97 °C. Nonetheless, these data clearly demonstrate that the reaction giving the *higher* stereoselectivity is *faster* than that giving the lower stereoselectivity.

7. Reactions of Deuterioalkoxide Complexes. We sought to rigorously establish the absolute configurations assigned above to the carbons in (+)-(*RR*)-**6a–f**-d_1. There are numerous means of determining absolute configurations of optically active primary deuterated alcohols HOCHDR and their derivatives. In particular, *O*-acetylmandelate esters $C_6H_5CH(OAc)COOCH_2R$ (**10**) corresponding to four of the six alkoxide complexes **6a–f** have been characterized previously (**10a–c,e**), and assignments of the diastereotopic methylene proton ^1H NMR resonances have been made in each case (H_R downfield of H_S for (−)-(*R*)-*O*-acetylmandelate esters in C_6D_6).[25b,29]

Hence, *racemic* deuterioalkoxide complexes (*RR*,*SS*)-**6a–f**-d_1 were treated with (−)-(*R*)-*O*-acetylmandelic acid, DMAP, and DCC as in Scheme III. Chromatography gave esters $C_6H_5CH(OAc)COOCHDR$ (**10a–f**-d_1) in 94–62% yields as 50:50 mixtures of (*RR*)/(*RS*) diastereomers (Scheme IV, entries 1–6). Compounds **10a–f**-d_1 were characterized by ^1H and $^{13}C\{^1H\}$ NMR, as described in the supplementary material (Table XI).[26] As expected, the −OCHD ^1H NMR resonances of the (*RR*)/(*RS*) diastereomers of **10a–c,e**-d_1 were well resolved (C_6D_6, 300 MHz). Those of **10d**-d_1 were resolved in C_6D_6 at 500 MHz with decoupling. Those of **10f**-d_1 were not resolved in C_6D_6 at 500 MHz but were resolved in acetone-d_6 with decoupling.

Next, optically active deuterioalkoxide complexes (+)-(*RR*)-**6a–f**-d_1 and (−)-(*R*)-$C_6H_5CH(OAc)COOH$ were similarly reacted (Scheme IV, entries 8–17). Chromatography gave esters (*RR*)-**10**-d_1 in diastereomeric purities that closely matched those of their precursors, as assayed by integration of the −OCHD ^1H NMR resonances. The downfield $-OCH_2$ ^1H NMR resonances of (*R*)-**10a–e** were absent in (*RR*)-**10a–e**-d_1, in accord with our configurational assignments. However, the upfield $-OCH_2$ ^1H NMR resonance of (*R*)-**10f** was absent in (*RR*)-**10f**-d_1. This was attributed to the solvent difference (acetone-d_6 vs C_6D_6), rather than an abrupt change in reaction stereochemistry.[29]

In some of the preceding experiments, the carboxylate complex byproducts (*RR*,*SR*)-**9** and (+)-(*RR*)-**9** were isolated as described in Scheme III. Yields ranged from 95% to 93%, and diastereomeric excesses (from experiments with (+)-(*RS*)-**3**$^+BF_4^-$) were >99%. Finally, some of the stereoselectivities in Scheme IV qualitatively differ from those previously reported for analogous reductions of PF_6^- salts.[12] We have not been able to reproduce

(29) Although logical assignments of the diastereotopic $-OCH_2$ ^1H NMR resonances in esters **10a–c,e** are made in ref 25b, these were verified by independent synthesis in only one case (**10c**-d_1). Thus, we performed the following additional checks. First, (+)-(*RR*)-**6a**-d_1 was converted by a similar procedure to a known (−)-camphanic acid ethanol-d_1 ester, which was assayed with NMR shift reagents as described previously (Gerlach, H.; Zagalak, B. *J. Chem. Soc., Chem. Commun.* **1973**, 274). Second, an authentic sample of (+)-(*S*)-$HOCHDC_6H_5$ was synthesized (Midland, M. M.; Greer, S.; Tramontano, A.; Zderic, S. A. *J. Am. Chem. Soc.* **1979**, *101*, 2352) and converted to (*RS*)-**10e**-d_1. Third, cyanide addition to (+)-(*RS*)-**3a,b,d–f**$^+BF_4^-$ was studied. NMR analyses of Mosher ester derivatives of the resulting cyanohydrin alkoxides showed the dominant addition stereochemistry to be the same in all cases, and identical with the deuteride addition stereochemistry in Scheme IV.[30]

(30) Garner, C. M.; Fernández, J. M.; Gladysz, J. A. *Tetrahedron Lett.* **1989**, *30*, 3931.

the somewhat higher de and ee values claimed earlier.

Discussion

1. Ground-State Binding Modes in Aldehyde Complexes. A variety of aldehyde (and ketone) complexes have been reported in the literature.[10,31,32] However, both σ and π complexes are common. Surprisingly, there have been few systematic studies of structure. Intuitively, metal fragments that are good π donors (such as I) should exhibit a greater propensity for π coordination. However, tests of this generalization are scarce. For example, an osmium η^2-acetone complex has been found to isomerize to an η^1-acetone complex upon one electron oxidation.[31a]

Naturally, the electronic and steric properties of aldehyde and ketone ligands should also influence the binding mode. For example, the π^* LUMO energies of formaldehyde, acetaldehyde, and acetone have been calculated to be 4.01, 4.39, and 4.53 eV, respectively.[33] Hence, formaldehyde is a better π acceptor than substituted aldehydes and should exhibit a greater propensity for π coordination. Accordingly, all isolable transition metal–formaldehyde complexes are π, whereas many substituted aldehyde complexes are σ.[10] Also, σ binding directs the carbonyl carbon and one substituent away from the metal fragment, whereas with π binding the carbonyl carbon and both substituents are held in closer proximity. Hence, steric effects also can bias substituted aldehydes and ketones toward σ coordination.

As expected from the preceding considerations, the carbon–oxygen bonds in propionaldehyde complex (*RS,SR*)-**3b**$^+BF_4^-$ (1.256 (14) Å) and phenylacetaldehyde complex (*RS,SR*)-**3f**$^+PF_6^-\cdot(CH_2Cl_2)_{0.5}$ (1.318 (11) Å) are much shorter than that in formaldehyde complex **4**$^+PF_6^-$ (Figure 4; 1.37 (2) Å). This indicates a significant diminution of backbonding or (in valence bond terms) a reduced contribution from a metallaoxacyclopropane resonance form. The carbon–oxygen bond lengths in formaldehyde and methanol are 1.203 and 1.43 Å, respectively.[34] Hence, the C–O bond orders in the substituted aldehyde complexes are in the range 1.5–1.8. Structural features of the corresponding ketone complexes, all of which exhibit a σ ground state, are analyzed in detail elsewhere.[20]

As noted above, only aromatic aldehyde complexes $[(\eta^5\text{-}C_5H_5)Re(NO)(PPh_3)(O{=}CHAr)]^+X^-$ have to date been found to exhibit appreciable equilibrium quantities of both π and σ isomers.[16] We speculate that aryl ring/carbonyl group conjugation is enhanced in the σ binding mode. Analogous resonance stabilization would not be available to aliphatic aldehyde ligands. Indeed, π/σ equilibria have been previously observed in selenobenzaldehyde, azobenzene, and related metal complexes.[35]

As shown in Figure 4, the aldehyde ligands in **4**$^+PF_6^-$, (*RS,SR*)-**3b**$^+BF_4^-$, and (*RS,SR*)-**3f**$^+PF_6^-\cdot(CH_2Cl_2)_{0.5}$ are not bound to the rhenium fragment I symmetrically but are "slipped", with the rhenium closer to oxygen. Significant C=C slippage is not observed in the crystal structures of analogous monosubstituted alkene complexes (Figure 4a).[22a,b] For comparison purposes, we calculate a "degree of slippage" as follows: first, define the point X (Figure 4) that is the intercept of the perpendicular from rhenium with the C–O (or C–C) bond; second, divide the displacement of point X from the *midpoint* of the C–O (or C–C) bond by *half* the C–O (or C–C) as a percentage.[36]

Application of the preceding algorithm indicates that the slippage of the aldehyde ligands in (*RS,SR*)-**3b**$^+BF_4^-$ and (*RS,SR*)-**3f**$^+PF_6^-\cdot(CH_2Cl_2)_{0.5}$ is 37% and 23%, respectively. This is much greater than the slippage of the formaldehyde ligand in **4**$^+PF_6^-$ (16%) or that of the monosubstituted alkene ligand in Figure 4a (1%). Thus, the successive replacement of the formaldehyde ligand hydrogens of **4**$^+PF_6^-$ by carbocation-stabilizing substituents effects progressively more slippage and ultimately, with ketones or certain aromatic aldehydes, a thermodynamic preference for σ binding.

2. Dynamic Equilibria in Aldehyde Complexes. Aldehyde complexes **3**$^+X^-$ can conceivably exhibit several types of dynamic equilibria. In addition to π/σ isomerization as analyzed above, two π diastereomers are possible (Figure 1): III (*RS,SR*) and IV (*RR,SS*). Complexes (*RS,SR*)-**3b**$^+BF_4^-$ and (*RS,SR*)-**3f**$^+PF_6^-\cdot(CH_2Cl_2)_{0.5}$ are diastereomerically pure in the solid state, and data given above strongly suggest that analogous (type III) diastereomers greatly predominate for all aldehyde complexes **3**$^+X^-$ in solution.

However, our present data do not rule out the rapid equilibration of (*RS,SR*)-**3**$^+X^-$ with small quantities of the opposite (type IV) diastereomers, (*RR,SS*)-**3**$^+X^-$. Although this complex issue will be analyzed in detail in a subsequent paper,[16] a possible equilibration mechanism is illustrated at this time (Scheme V). Since aldehyde ligand dissociation is slow, we suggest that π diastereomers might interconvert via σ intermediates such as *E*-V. Isomer *E*-V is depicted with a rhenium–oxygen conformation close to those found in crystal structures of corresponding σ-ketone complexes,[20] although other rotamers such as VI (Scheme V) may be similar in energy. Note that a C=O geometric isomer, *Z*-V, can also exist. However, *Z*-V is likely less stable than *E*-V due to the cis relationship of the aldehyde substituent and the rhenium moiety.

Scheme V. Possible Mechanism for Interconversion of Aldehyde Complex Diastereomers

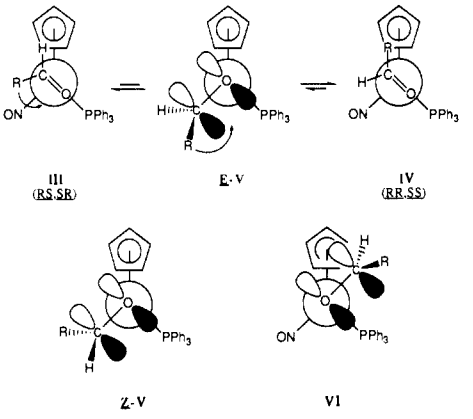

(31) Some key papers on transition-metal–aldehyde complexes that have appeared since the publication of ref 10: (a) Harman, W. D.; Sekine, M.; Taube, H. *J. Am. Chem. Soc.* **1988**, *110*, 2439. (b) Birk, R.; Berke, H.; Hund. H.-U.; Evertz, K.; Huttner, G.; Zsolnai, L. *J. Organomet. Chem.* **1988**, *342*, 67. (c) Bullock, R. M.; Rappoli, B. J.; Samsel, E. G.; Rheingold, A. L. *J. Chem. Soc., Chem. Commun.* **1989**, 261. (d) Bullock, R. M.; Ricci, J. S.; Szalda, D. J. *J. Am. Chem. Soc.* **1989**, *111*, 2741. (e) Bonnesen, P. V.; Puckett, C. L.; Honeychuck, R. V.; Hersh, W. H. *Ibid.* **1989**, *111*, 6070. (f) Bryan, J. C.; Mayer, J. M. *Ibid.* **1990**, *112*, 2298.

(32) Some key papers on main group element–aldehyde complexes: (a) Reetz, M. T.; Hüllmann, M.; Massa, W.; Berger, S.; Rademacher, P.; Heymanns, P. *J. Am. Chem. Soc.* **1986**, *108*, 2405. (b) Keck, G. E.; Castellino, S. *Ibid.* **1986**, *108*, 3847. (c) Denmark, S. E.; Henke, B. R.; Weber, E. *Ibid.* **1987**, *109*, 2512. (d) Maruoka, K.; Araki, Y.; Yamamoto, H. *Ibid.* **1988**, *110*, 2650. (e) LePage. T. J.; Wiberg, K. B. *Ibid.* **1988**, *110*, 6642.

(33) (a) Calculated energies of potential donor orbitals of formaldehyde, acetaldehyde, and acetone are as follows (eV): π, −14.33, −13.46, −13.00; *n*, −11.78, −11.31, −10.93; Wu, Y.-O.; Houk, K. N. Unpublished results, UCLA. (b) Note that ligand rehybridization occurs upon π complexation, moderately affecting the frontier orbital energies.

(34) (a) March, J. *Advced Organic Chemistry*; Wiley: New York, 1985; p 19. (b) Streitwieser, A., Jr.; Heathcock, C. H. *Introduction to Organic Chemistry*, 3rd ed.; Macmillan: New York, 1985; pp 188 and 357.

(35) (a) Fischer, H.; Zeuner, S.; Riede, J. *Angew. Chem., Int. Ed. Engl.* **1984**, *23*, 726. (b) Fischer, H.; Zeuner, S.; Gerbing, U.; Kreiter, C. G. *J. Organomet. Chem.* **1989**, *377*, 105. (c) Schenk, W. A.; Rüb, D.; Burschka, C. *Ibid.* **1987**, *328*, 287. (d) Einstein, F. W. B.; Sutton, D.; Tyers, K. G. *Inorg. Chem.* **1987**, *26*, 111.

(36) (a) This formula reduces to two limits: 0% slippage when the perpendicular intercepts the C–O (C–C) bond midpoint, and 100% slippage when ∠C–O–Re(or O–C–Re) = 90°. (b) Geometries of alkene complexes have been analyzed in detail: Ittel, S. D.; Ibers, J. A. *Adv. Organomet. Chem.* **1976**, *14*, 33. Several alternative protocols exist for quantifying features associated with M–C–X planes. (c) It should be emphasized that the comparison of features of Re–C–X planes in separate molecules (e.g., angles with bonds) can be complicated by secondary distortions from idealized structures of the types II/III. We have performed several checks that indicate any such factors cancel.

There is an apparent paradox in the preceding proposal. The ^1H NMR spectrum of formaldehyde complex $\mathbf{4}^+PF_6^-$ exhibits *two* distinct formaldehyde proton resonances that do not decoalesce at 100 °C.[19] This bounds $\Delta G^{\ddagger}_{100°C}$ for any process capable of exchanging the protons, such as a $\pi \rightarrow \sigma \rightarrow \pi$ isomerization, as >17.5 kcal/mol. However, in the previous section we noted that the structure of $\mathbf{4}^+PF_6^-$ exhibits considerably more "metallaoxacyclopropane character" than (RS,SR)-$\mathbf{3b}^+BF_4^-$ and (RS,SR)-$\mathbf{3f}^+PF_6^-\cdot(CH_2Cl_2)_{0.5}$. Further, $\mathbf{4}^+PF_6^-$ should on electronic and steric grounds exhibit a greater ΔG for equilibration to a σ isomer. Hence, we believe it reasonable to propose that the equilibria in Scheme V would be rapid for $\mathbf{3}^+X^-$ but much slower for $\mathbf{4}^+PF_6^-$.

3. Transition-State Structures for Aldehyde Ligand Reduction. Given the diverse binding options for aldehyde ligands outlined above, a variety of mechanisms must be considered for the reduction of (RS,SR)-$\mathbf{3}^+X^-$ by formyl complex **5**. One possibility is a concerted reduction, without any pre-equilibrium isomerizations. Both experimental and theoretical studies have shown that slippage can activate π ligands toward nucleophilic attack.[4b,c] Accordingly, aldehyde complexes (RS,SR)-$\mathbf{3}^+X^-$ are much more reactive than free aldehydes toward **5**. However, the possibility that σ isomers of (RS,SR)-$\mathbf{3}^+X^-$ are the kinetically active species must be considered. We are not aware of any experimental or theoretical studies of the relative reactivities of σ and π aldehyde complexes toward nucleophiles. However, recent theoretical work seems to imply that σ complexes should be more reactive.[32e] Intuitively, the σ binding mode should impart a greater polarization and electrophilicity to the C=O bond.

To the extent that two diastereomeric deuteride addition products are obtained in Scheme IV, two isomeric transition states must be operative. First consider possible π transition states. The major products in Scheme IV can be derived from *net* deuteride attack on the aldehyde face anti to the rhenium, and the minor products can be derived from *net* deuteride attack on the aldehyde face syn to the rhenium.

It has been previously proposed from theoretical studies that the nitrosyl ligand might mediate hydride additions to the carbonyl ligand of $[(\eta^5\text{-}C_5H_5)Re(NO)(PPh_3)(CO)]^+X^-$.[37] Such a mechanism would deliver deuteride syn to the rhenium in (RS,SR)-$\mathbf{3}^+X^-$ and generate the minor diastereomers in Scheme IV. However, we have never observed NMR evidence for nucleophile/nitrosyl ligand adducts. Further, the two diastereomers of monosubstituted alkene complexes $[(\eta^5\text{-}C_5H_5)Re(NO)(PPh_3)(H_2C{=}CHR)]^+X^-$ each undergo stereospecific addition of alkyl copper reagents from a direction anti to rhenium.[38] Hence, we disfavor at this time all syn attack mechanisms.

Another mechanism that would give the minor diastereomers in Scheme IV involves initial generation of the less stable aldehyde complex diastereomers (RR,SS)-$\mathbf{3}^+X^-$ (IV, Scheme V), followed by deuteride attack on the aldehyde face anti to the rhenium. A conceptually related mechanism dominates in the rhodium-catalyzed asymmetric hydrogenation of alkenes.[39] As an indirect probe of this possibility, we synthesized *pentamethyl*cyclopentadienyl analogues of (RS,SR)-$\mathbf{3a,b,d\text{-}f}^+BF_4^-$, (RS,SR)-$[(\eta^5\text{-}C_5Me_5)Re(NO)(PPh_3)(\eta^2\text{-}O{=}CHR)]^+BF_4^-$. We thought that the added bulk of the C_5R_5 ligand would disfavor π diastereomers corresponding to IV, diminishing equilibrium concentrations. However, the diastereoselectivities observed in reductions with racemic $\mathbf{5}\text{-}d_1$ were only very slightly higher.[40] This suggests that the minor products in Scheme IV are formed by other pathways.

Mechanisms involving the intermediacy of σ complexes such as V (Scheme V) provide intuitively satisfying routes to both product diastereomers in Scheme IV. Deuteride attack upon the carbonyl carbon in *E*-V from a direction anti to the bulky PPh_3 ligand would give the major product diastereomers. The minor diastereomers could form by several routes: (1) attack upon the carbonyl carbon in *E*-V from a direction syn to the PPh_3 ligand, (2) attack upon the carbonyl carbon in geometric isomer *Z*-V from a direction anti to the PPh_3 ligand, and (3) attack upon the carbonyl carbon in the rhenium–oxygen bond rotamer of *E*-V, VI, from a direction anti to the PPh_3 ligand.

Although conclusions cannot be made on the basis of the present data, we expect that future experiments will provide support for the intermediacy of σ complexes in nucleophilic additions to (RS,SR)-$\mathbf{3}^+X^-$.[41] Interestingly, σ-methyl ketone complexes (E)-$[(\eta^5\text{-}C_5H_5)Re(NO)(PPh_3)(\eta^1\text{-}O{=}C(R)CH_3)]^+X^-$ and formyl complex **5** react to give secondary alkoxide complexes $(\eta^5\text{-}C_5H_5)Re(NO)(PPh_3)(OCH(R)CH_3)$ in diastereomer ratios similar to those obtained in Scheme IV.[20] The dominant stereochemistry is consistent with attack upon the carbonyl carbon in a rotamer analogous to *E*-V from a direction anti to the PPh_3 ligand.

4. Trends in Reduction Stereoselectivities. There are several interesting trends in the stereoselectivities summarized in Scheme IV, some of which bear upon the deuteride addition transition states. In interpreting these, it should be emphasized that nearly all reactions utilized 0.98–1.02 equiv (i.e., essentially 1 equiv) of deuterioformyl complex $\mathbf{5}\text{-}d_1$. Thus, both enantiomers of a racemic reactant are consumed during a reaction.

First, optically active aldehyde complexes (+)-(RS)-$\mathbf{3}^+BF_4^-$ are reduced with higher stereoselectivities by formyl complex (+)-(S)-$\mathbf{5}\text{-}d_1$ than enantiomer (−)-(R)-$\mathbf{5}\text{-}d_1$. In other words, the first pair of reactants "match up" better, giving deuterioalkoxide complexes (+)-(RR)-$\mathbf{6}\text{-}d_1$ in greater diastereomeric excesses. Intermediate stereoselectivities would be expected with $\mathbf{5}\text{-}d_1$ that was not optically pure. Accordingly, the reduction of (+)-(RS)-$\mathbf{3e}^+BF_4^-$ by *racemic* $\mathbf{5}\text{-}d_1$ (Scheme IV, entry 7) gives (+)-(RR)-$\mathbf{6}\text{-}d_1$ in 85% de—the average of the de obtained with (+)-(S)-$\mathbf{5}\text{-}d_1$ and (−)-(R)-$\mathbf{5}\text{-}d_1$.

At present, we do not have a mechanistic rationale for this commonly observed *type* of phenomenon.[28] However, methyl ketone complexes (+)-(R)-$[(\eta^5\text{-}C_5H_5)Re(NO)(PPh_3)(\eta^1\text{-}O{=}C(R)CH_3)]^+X^-$ are also reduced with considerably higher stereoselectivities by (+)-(S)-$\mathbf{5}\text{-}d_1$ than (−)-(R)-$\mathbf{5}\text{-}d_1$.[20b] This suggests that both classes of substrates react with formyl complex **5** via a common mechanism.

Interestingly, the series of experiments with *racemic* aldehyde complexes (RS,SR)-$\mathbf{3}^+BF_4^-$ and *racemic* formyl complex $\mathbf{5}\text{-}d_1$ gives stereoselectivities that are *higher* than the averages of those obtained with the two enantiomers of $\mathbf{5}\text{-}d_1$. This follows from the observation that the reaction of (+)-(RS)-$\mathbf{3e}^+BF_4^-$ and (+)-(S)-$\mathbf{5}\text{-}d_1$ is *faster* than that of (+)-(RS)-$\mathbf{3e}^+BF_4^-$ and enantiomer (−)-(R)-$\mathbf{5}\text{-}d_1$. When both reactants are racemic, there are four possible chirality combinations ($\mathbf{3}^+BF_4^-/\mathbf{5}\text{-}d_1$ = RS/S, RS/R, SR/S, SR/R). The two that react the most quickly (RS/S, SR/R) give the higher stereoselectivities, and lead to different enantiomers of the *same* diastereomer.

5. Applications to Organic Synthesis. Scheme IV provides a very general and stereoselective entry into derivatives of chiral α-deuterio primary alcohols. On the basis of these criteria, it compares favorably with other chemical methodologies developed to date.[4c,42] However, some practical limitations are apparent: (1) stoichiometric quantities of a moderately expensive metal are utilized, and (2) the reductant is not commercially available and requires exacting preparative conditions. Nonetheless, the design principles that underlie this chemistry offer considerable flexibility. Variations that address these limitations are readily envisioned.

The results in Scheme IV can also be extended to other nucleophiles. For example, cyanide adds to (RS,SR)-$\mathbf{3}^+BF_4^-$ in high yields to give cyanohydrin alkoxide complexes $(\eta^5\text{-}C_5H_5)Re$-

(37) Fenske, R. F.; Milletti, M. C. *Organometallics* **1986**, *5*, 1243.
(38) Peng, T.-S.; Gladysz, J. A. Submitted for publication.
(39) Landis, C. R.; Halpern, J. *J. Am. Chem. Soc.* **1987**, *109*, 1746.
(40) Agbossou, F. N.; Ramsden, J. A.; Huang, Y.-H.; Arif, A. M.; Gladysz, J. A. Manuscript in preparation.

(41) Nucleophilic additions to η^1-aldehyde complexes might be distinguished by inverse secondary deuterium kinetic isotope effects ($k_{O=CHR}/k_{O=CDR}$). The rapid reactions described in this paper are not ideal for the extensive rate studies this would require.
(42) Arigoni, D.; Eliel, E. L. *Top. Stereochem.* **1969**, *4*, 127.

$(NO)(PPh_3)(OCH(CN)R)$ as 95–76:5–24 mixtures of diastereomers.[30] The dominant stereochemistry is analogous to that in Scheme IV. However, the stereoselectivities are somewhat lower, particularly with acetaldehyde complex (*RS*,*SR*)-**3a**$^+BF_4^-$. This might reflect the reduced bulk of the attacking nucleophile or the absence of the stereoselectivity-enhancing effect available to the chiral reductant **5**.

An advantage of our methodology is that the alkoxide complexes generated are versatile intermediates (Scheme III). The alkoxide ligand lone pairs exhibit enhanced basicity and nucleophilicity.[43,44] Consequently, reactions with electrophiles E^+X^- occur readily. We have described elsewhere stoichiometric protonations of alkoxide complexes **6** to isolable alcohol complexes $[(\eta^5\text{-}C_5H_5)\text{-}Re(NO)(PPh_3)(HOCH_2R)]^+BF_4^-$[44] and alkylations to isolable ether complexes $[(\eta^5\text{-}C_5H_5)Re(NO)(PPh_3)(ROCH_2R)]^+X^-$.[43] We presume that analogous species are intermediates in all of the transformations in Scheme III.

The reactions in Scheme III give easily isolated rhenium byproducts $(\eta^5\text{-}C_5H_5)Re(NO)(PPh_3)(X)$ in high optical yields. Procedures for the conversion of these species to optically active carbonyl complex $[(\eta^5\text{-}C_5H_5)Re(NO)(PPh_3)(CO)]^+X^-$ and methyl complex **1** have been described.[17] However, eq 4 of Scheme III provides the best means of recycling the rhenium auxiliary. Here, alkoxide complex (+)-(*R*)-**6e** is reacted with an acid with a "noncoordinating" counteranion, and subsequent addition of an aldehyde liberates the alcohol product and regenerates the original aldehyde complex in high chemical and optical yield. It is easy to visualize reactions of aldehydes and certain nucleophiles (e.g., those that contain transferable electrophilic moieties) that would be truly catalytic in rhenium. Research toward this objective is in progress.

Elegant synthetic studies of several other investigators are particularly relevant to this research. First, Faller has recently reported a class of chiral, optically active molybdenum allyl complexes that react with aldehydes in the presence of methanol to give homoallylic alcohols in high chemical and optical yields (eq 5).[5a,b] These stoichiometric transformations are believed to involve an intermediate σ-aldehyde complex **11**. Related reactions of chiral titanium allyl complexes have also been described.[5c]

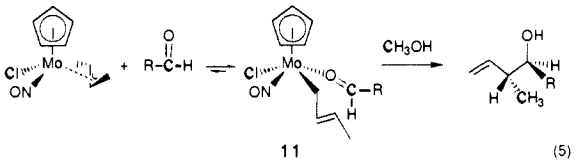

11 (5)

A variety of chiral amines *catalyze* the asymmetric addition of alkyl zinc reagents to aldehydes.[2] Zinc/amine σ-aldehyde complexes have been detected by ^1H NMR under the reaction conditions.[2a] Similarly, a chiral iron/gold(I) complex catalyzes a highly efficient asymmetric aldol reaction of aldehydes and α-isocyanoacetates.[3] Gold σ-aldehyde complexes have been proposed as intermediates. Hence, chiral metal complexes show exceptional and increasing utility as reagents or catalysts for a broad spectrum of asymmetric transformations of aldehydes.

6. Summary and Conclusions. The chiral Lewis acid $[(\eta^5\text{-}C_5H_5)Re(NO)(PPh_3)]^+$ serves as an effective template for the stereoselective binding and reduction of aldehydes. Although the dominant binding mode (π) has been identified, further studies are needed to quantify equilibria with σ and other types of isomers. Several types of transition states remain possible for aldehyde ligand reduction. However, stereochemistry is in all cases easily rationalized.

The alkoxide ligand in reduction products **6** can be liberated by a variety of methods, and with preservation of stereochemistry at rhenium. Hence, the rhenium chiral auxiliary can be recycled without additional optical resolution. These protocols have not been optimized, and appropriate aldehyde/nucleophile combinations may allow rhenium to be employed in catalytic quantities. Further data pertaining to these synthetic and mechanistic issues, as well as detailed studies of analogous methyl ketone[20c] and aromatic aldehyde[16a] complexes, will be reported in the near future.

Experimental Section

General Methods. General procedures recently have been described.[11] All GC analyses were conducted on a Hewlett Packard 5890A chromatograph. The ^1H NOED NMR experiments were conducted as detailed previously.[9c]

Solvents were purified as follows: hexane, distilled from Na/benzophenone; benzene, filtered through activated alumina and distilled from Na/benzophenone; ether and THF, distilled from $LiAlH_4$ and then Na/benzophenone; pentane, heptane, and toluene, distilled from Na; CH_2Cl_2, distilled from P_2O_5 or CaH_2; ethyl acetate, used as received; C_6D_6 and CD_2Cl_2, vacuum transferred from CaH_2; D_2O (Cambridge Isotope Laboratories, 99.9% labeled), vacuum degassed. Florisil was treated with concentrated NH_4OH (30% v/w), and silica (230–400 mesh) was used as received.

Acids $HBF_4{\cdot}O(C_2H_5)_2$ (Aldrich) and $HPF_6{\cdot}O(C_2H_5)_2$ (Columbia) were standardized as described previously.[11] Aldehydes were obtained from common commercial sources and were fractionally distilled. Reagents HI (47% aqueous, Fisher), $(CH_3)_3SiI$, DCC, DMAP, (+)-$Eu(hfc)_3$ (Aldrich), and CH_3COI (Pfaltz and Bauer) were used as received. (−)-(*R*)- and (+)-(*S*)-*O*-acetylmandelic acids (Aldrich) were used as received, converted to the corresponding (−)-menthyl (and (±)-menthyl) esters by procedures similar to one previously described,[25c] and shown to be 99.5% and 95.3% ee, respectively, by capillary GC analysis (0.2 mm × 25 m SE-54 column, 170 → 250 °C at 3 deg/min; ester retention times 18.22 and 17.93 min, respectively). NaD_4 (Aldrich, 98.8% labeled per lot assay) was used as received. Benzaldehyde-d_1 was prepared from methyl benzoate (Fisher) by standard $LiAlD_4$ reduction/PCC oxidation procedures.[45]

Preparation of $[(\eta^5\text{-}C_5H_5)Re(NO)(PPh_3)(\eta^2\text{-}O{=}CHCH_3)]^+X^-$ (3a$^+X^-$). A. Methyl complex $(\eta^5\text{-}C_5H_5)Re(NO)(PPh_3)(CH_3)$ (**1**,[13] 0.333 g, 0.596 mmol), CH_2Cl_2 (ca. 25 mL), and $HPF_6{\cdot}O(C_2H_5)_2$ (0.044 mL, 0.596 mmol) were combined at −80 °C to give $[(\eta^5\text{-}C_5H_5)Re(NO)(PPh_3)(ClCH_2Cl)]^+PF_6^-$ (**2**) as previously described.[11] Then acetaldehyde (0.099 mL, 1.77 mmol; 3 equiv) was added with stirring. The solution was allowed to slowly warm to room temperature. After 0.5 h, the solution was concentrated to ca. 5 mL. A yellow powder formed, and ether was added with stirring to effect further precipitation. The powder was collected by filtration, washed with 50:50 (v/v) ether/CH_2Cl_2, and dried under oil pump vacuum to give yellow microcrystalline (*RS*,*SR*)-**3a**$^+PF_6^-$ (0.398 g, 0.543 mmol, 91%), mp 178–181 °C dec. Anal. Calcd for $C_{25}H_{24}F_6NO_2P_2Re$: C, 40.99; H, 3.30. Found: C, 40.90; H, 3.49. B. Tetrafluoroborate salt (*RS*,*SR*)-**3a**$^+BF_4^-$ was analogously obtained as a tan powder (96%), mp 205–206 °C dec. Anal. Calcd for $C_{25}H_{24}BF_4NO_2PRe$: C, 44.52; H, 3.59. Found: C, 44.31; H, 3.58. C. Optically active methyl complex (+)-(*S*)-**1** (0.206 g, 0.368 mmol),[8] CH_2Cl_2 (4 mL), $HBF_4{\cdot}O(C_2H_5)_2$ (0.055 mL, 0.405 mmol), and acetaldehyde (0.103 mL, 1.84 mmol, 5 equiv) were combined in a procedure analogous to that given for (*RS*,*SR*)-**3a**$^+PF_6^-$. After 10 min, the flask was transferred to a 0 °C bath, and stirring was continued. Then ether (20–30 mL) was added to precipitate a tan powder (any oil formed was triturated to a powder), which was collected by filtration, washed with ether, and dried under oil pump vacuum to give (+)-(*RS*)-**3a**$^+BF_4^-$ (0.232 g, 0.344 mmol, 94%), mp 190–191 °C dec, $[\alpha]^{25}_{589}$ 55 ± 4°.[15] Anal. Found (two preparations): C, 44.35, 44.40; H, 3.56, 3.64.

Preparation of $[(\eta^5\text{-}C_5H_5)Re(NO)(PPh_3)(\eta^2\text{-}O{=}CHCH_2CH_3)]^+X^-$ (3b$^+X^-$). A. Complex **1** (0.403 g, 0.721 mmol), CH_2Cl_2 (ca. 15 mL), $HPF_6{\cdot}O(C_2H_5)_2$ (0.053 mL, 0.712 mmol), and propionaldehyde (0.153 mL, 2.1 mmol) were combined in a procedure analogous to that given for (*RS*,*SR*)-**3a**$^+PF_6^-$. The dark yellow powder that precipitated was extracted with CH_2Cl_2 (2–3 mL). Ether was slowly added by vapor diffusion. Yellow plates formed, which were collected by filtration and dried in vacuo to give (*RS*,*SR*)-**3b**$^+PF_6^-$ (0.413 g, 0.553 mmol, 77%), mp 193–196 °C dec. Anal. Calcd for $C_{26}H_{26}F_6NO_2P_2Re$: C, 41.83; H, 3.51. Found: C, 42.06; H, 3.68. B. Tetrafluoroborate salt (*RS*,*SR*)-**3b**$^+BF_4^-$ was analogously obtained as a light yellow powder (92%), mp 203–206 °C dec. Anal. Calcd for $C_{26}H_{26}BF_4NO_2PRe$: C, 45.36; H, 3.81. Found: C, 45.23; H, 3.75. A sample was dissolved in CH_2Cl_2, and a layer of ether was added. This gave bronze crystals, mp 200–204 °C dec. Anal. Found: C, 45.27; H, 3.94. C. Methyl complex (+)-(*S*)-**1** (0.234 g, 0.419 mmol), CH_2Cl_2 (4 mL), $HBF_4{\cdot}O(C_2H_5)_2$ (0.063 mL, 0.461 mmol) and propionaldehyde (0.151 mL, 2.1 mmol) were combined

(43) Agbossou, S. K.; Fernández, J. M.; Gladysz, J. A. *Inorg. Chem.* **1990**, *29*, 476.
(44) Agbossou, S. K.; Smith, W. W.; Gladysz, J. A. *Chem. Ber.* In press.
(45) (a) Fetizon, M.; Henry, Y.; Moreau, N.; Moreau, G.; Golfier, M.; Prange, T. *Tetrahedron* **1973**, *29*, 1011. (b) Corey, E. J.; Suggs, J. W. *Tetrahedron Lett.* **1975**, *16*, 2647.

in a procedure analogous to that given for (+)-(*RS*)-**3a**$^+BF_4^-$. An identical workup gave (+)-(*RS*)-**3b**$^+BF_4^-$ (0.260 g, 0.378 mmol, 90%) as a light yellow powder, mp 191–194 °C dec, $[\alpha]^{25}_{589}$ 48 ± 1°.[15] Anal. Found: C, 45.12; H, 3.78.

Preparation of $[(\eta^5\text{-}C_5H_5)Re(NO)(PPh_3)(\eta^2\text{-}O{=}CH\text{-}CH_2CH_2CH_3)]^+X^-$ (3c$^+$X$^-$). A. Complex **1** (0.237 g, 0.424 mmol), CH_2Cl_2 (ca. 25 mL), $HPF_6{\cdot}O(C_2H_5)_2$ (0.032 mL, 0.416 mmol), and butyraldehyde (0.115 mL, 1.3 mmol) were combined in a procedure analogous to that given for (*RS*,*SR*)-**3b**$^+PF_6^-$. An identical workup gave yellow plates of (*RS*,*SR*)-**3c**$^+PF_6^-$ (0.263 g, 0.346 mmol, 82%), mp 178–182 °C dec. Anal. Calcd for $C_{27}H_{28}F_6NO_2P_2Re$: C, 42.63; H, 3.71. Found: C, 42.45; H, 3.81. B. Tetrafluoroborate salt (*RS*,*SR*)-**3c**$^+BF_4^-$ was analogously obtained as bronze plates from layered CH_2Cl_2/pentane (87%), mp 174–178 °C dec. Anal. Calcd for $C_{27}H_{28}BF_4NO_2PRe$: C, 46.16; H, 4.02. Found: C, 45.66; H, 3.97. C. Methyl complex (+)-(*S*)-**1** (0.208 g, 0.373 mmol), CH_2Cl_2 (4 mL), $HBF_4{\cdot}O(C_2H_5)_2$ (0.056 mL, 0.410 mmol), and butyraldehyde (0.165 mL, 1.86 mmol) were combined in a procedure analogous to that given for (+)-(*RS*)-**3a**$^+BF_4^-$. The reaction mixture was slowly added to ether (100 mL) with stirring. A precipitate slowly formed, which was collected by filtration and dried under vacuum to give (+)-(*RS*)-**3c**$^+BF_4^-$ (0.148 g, 0.211 mmol, 57%) as a yellow powder, mp 179–182 °C dec, $[\alpha]^{25}_{589}$ 56 ± 6°.[15] Anal. Found: C, 45.92, H, 4.07.

Preparation of $[(\eta^5\text{-}C_5H_5)Re(NO)(PPh_3)(\eta^2\text{-}O{=}CHCH(CH_3)_2)]^+X^-$ (3d$^+$X$^-$). A. Complex **1** (0.456 g, 0.816 mmol), CH_2Cl_2 (ca. 40 mL), $HPF_6{\cdot}O(C_2H_5)_2$ (0.063 mL, 0.814 mmol), and isobutyraldehyde (0.221 mL, 2.4 mmol) were combined in a procedure analogous to that given for (*RS*,*SR*)-**3b**$^+PF_6^-$. An identical workup gave yellow plates of (*RS*,*SR*)-**3d**$^+PF_6^-$ (0.491 g, 0.646 mmol, 79%), mp 182–185 °C dec. Anal. Calcd for $C_{27}H_{28}F_6NO_2P_2Re$: C, 42.63; H, 3.71. Found: C, 42.58; H, 3.41. B. Tetrafluoroborate salt (*RS*,*SR*)-**3d**$^+BF_4^-$ was obtained as a tan powder (94%), mp 202–207 °C dec, by a procedure similar to that given for (*RS*,*SR*)-**3a**$^+PF_6^-$, except that ether washings were used. Anal. Calcd for $C_{27}H_{28}BF_4NO_2PRe$: C, 46.16; H, 4.02. Found (two preparations): C, 46.00, 45.97; H, 3.96, 3.82. A sample was dissolved in CH_2Cl_2, and ether was added by vapor diffusion. Bronze plates formed, which were collected by filtration and dried under vacuum, mp 204–209 °C dec. Anal. Found: C, 46.00; H, 3.97. C. Methyl complex (+)-(*S*)-**1** (0.211 g, 0.377 mmol), CH_2Cl_2 (4 mL), $HBF_4{\cdot}O(C_2H_5)_2$ (0.057 mL, 0.415 mmol), and isobutyraldehyde (0.171 mL, 1.89 mmol) were combined in a procedure analogous to that given for (+)-(*RS*)-**3a**$^+BF_4^-$. An identical workup gave (+)-(*RS*)-**3d**$^+BF_4^-$ (0.188 g, 0.268 mmol, 71%) as a dark tan powder, mp 192–198 °C dec, $[\alpha]^{25}_{589}$ 42 ± 2°.[15] Anal. Found: C, 45.96; H, 4.07.

Preparation of $[(\eta^5\text{-}C_5H_5)Re(NO)(PPh_3)(\eta^2\text{-}O{=}CHC_6H_5)]^+X^-$ (3e$^+$X$^-$). A. Complex **1** (0.287 g, 0.514 mmol), CH_2Cl_2 (ca. 25 mL), $HPF_6{\cdot}O(C_2H_5)_2$ (0.037 mL, 0.504 mmol), and benzaldehyde (0.153 mL, 1.50 mmol) were combined in a procedure analogous to that given for (*RS*,*SR*)-**3a**$^+PF_6^-$. An identical workup gave (*RS*,*SR*)-**3e**$^+PF_6^-$ as a yellow microcrystalline powder (0.363 g, 0.457 mmol, 89%), mp 201–205 °C dec. Anal. Calcd for $C_{30}H_{26}F_6NO_2P_2Re$: C, 45.34; H, 3.30. Found: C, 45.56; H, 3.36. B. Tetrafluoroborate salt (*RS*,*SR*)-**3e**$^+BF_4^-$ was analogously obtained as a bright yellow powder (98%), mp 201–205 °C dec. Anal. Calcd for $C_{30}H_{26}BF_4NO_2PRe$: C, 48.92; H, 3.56. Found (three preparations): C, 48.85, 48.84, 48.68; H, 3.56, 3.56, 3.58. C. Methyl complex (+)-(*S*)-**1** (0.207 g, 0.370 mmol), CH_2Cl_2 (4 mL), $HBF_4{\cdot}O(C_2H_5)_2$ (0.056 mL, 0.407 mmol), and benzaldehyde (0.188 mL, 1.85 mmol) were combined in a procedure analogous to that given for (+)-(*RS*)-**3a**$^+BF_4^-$. An identical workup gave (+)-(*RS*)-**3e**$^+BF_4^-$ (0.259 g, 0.352 mmol, 95%) as a bright yellow powder, mp 189–193 °C dec, $[\alpha]^{25}_{589}$ 316 ± 3°.[15] Anal. Found (two preparations): C, 48.79, 48.40; H, 3.55, 3.64.

Preparation of $[(\eta^5\text{-}C_5H_5)Re(NO)(PPh_3)(\eta^2\text{-}O{=}CHCH_2C_6H_5)]^+X^-$ (3f$^+$X$^-$). A. Complex **1** (0.531 g, 0.951 mmol), CH_2Cl_2 (ca. 25 mL), $HPF_6{\cdot}O(C_2H_5)_2$ (0.071 mL, 0.962 mmol), and phenylacetaldehyde (0.340 mL, 2.91 mmol) were combined in a procedure analogous to that given for (*RS*,*SR*)-**3b**$^+PF_6^-$. Either CH_2Cl_2/ether or CH_2Cl_2/hexane recrystallization gave (*RS*,*SR*)-**3f**$^+PF_6^-{\cdot}(CH_2Cl_2)_{0.5}$ as yellow plates (0.641 g, 0.753 mmol, 79%), mp 138–142 °C dec. The presence of the solvate was verified by ^{1}H NMR (δ 5.63 (s) vs $Si(CH_3)_4$, acetone-d_6). Anal. Calcd for $C_{31}H_{28}F_6NO_2P_2Re{\cdot}(CH_2Cl_2)_{0.5}$: C, 44.45; H, 3.43; Cl, 4.17. Found: from ether, C, 44.23, H, 3.64; from hexane, C, 44.24, H, 3.50, Cl, 4.22. B. Tetrafluoroborate salt (*RS*,*SR*)-**3f**$^+BF_4^-$ was analogously obtained as a tan powder (90%), mp 165–170 °C dec. Anal. Calcd for $C_{31}H_{28}BF_4NO_2PRe$: C, 49.61; H, 3.76. Found (two preparations): C, 49.33, 49.16; H, 3.82, 4.09. C. Methyl complex (+)-(*S*)-**1** (0.211 g, 0.377 mmol), CH_2Cl_2 (4 mL), $HBF_4{\cdot}O(C_2H_5)_2$ (0.057 mL, 0.415 mmol), and phenylacetaldehyde (0.221 mL, 1.89 mmol) were combined in a procedure analogous to that given for (+)-(*RS*)-**3a**$^+BF_4^-$. Solvent was removed under vacuum, and the residue was dissolved in CH_2Cl_2 (4 mL). This solution was added to ether (150 mL) with vigorous stirring. The resulting precipitate was collected by filtration, washed with ether, and dried under oil pump vacuum to give (+)-(*RS*)-**3f**$^+BF_4^-$ (0.241 g, 0.321 mmol, 85%) as a tan powder, mp 122–128 °C dec, $[\alpha]^{25}_{589}$ 73 ± 8°.[15] Anal. Found: C, 48.91; H, 3.83.

Preparation of $(\eta^5\text{-}C_5H_5)Re(NO)(PPh_3)(OCH_2CH_3)$ (6a). A. A Schlenk tube was charged with (*RS*,*SR*)-**3a**$^+BF_4^-$ (0.138 g, 0.205 mmol), formyl complex **5** (0.115 g, 0.201 mmol), and a stir bar. The tube was cooled to −80 °C, and CH_2Cl_2 (5 mL) was added. The resulting suspension was stirred for 2.5 h at −80 °C and then for 3 h at room temperature. Solvent was removed under oil pump vacuum and the residue was extracted with benzene (1 × 4 mL, 5 × 2 mL). The extracts were sequentially passed via cannula through a 1 × 3 cm column of deactivated Florisil in a Kramer filter.[46] Solvent was removed from the eluate under oil pump vacuum to give **6a** (0.106 g, 0.180 mmol, 90%) as a red-orange foam/oil, which was dissolved in benzene (ca. 2 mL). Hexane (ca. 30 mL) was added, and the sample was taken to dryness under oil pump vacuum to give **6a** as a dark orange powder, mp 156–162 °C dec. Anal. Calcd for $C_{25}H_{25}NO_2PRe$: C, 50.84; H, 4.27. Found: C, 50.76; H, 4.27. Crystallization from toluene/hexane (layered, −24 °C) gave **6a** as ruby red droplets, mp 159–167 °C dec. Anal. Found: C, 51.54; H, 4.39. B. Optically active (+)-(*RS*)-**3a**$^+BF_4^-$ (0.103 g, 0.153 mmol) and **5** (0.085 g, 0.148 mmol) were reacted similarly (4 mL CH_2Cl_2, 1.5 h at −80 °C and 1.5 h at 0 °C). Solvent was removed under oil pump vacuum, and the residue was extracted with benzene (1 × 4 mL, 3 × 2 mL). The extracts were chromatographed as above, and the eluate was concentrated to ca. 1 mL. Then hexane (10 mL) was added. The sample was taken to dryness under oil pump vacuum to give (+)-(*R*)-**6a** (0.080 g, 0.136 mmol, 92%) as a red-orange foam/oil. For analytical data, the foam/oil was dissolved in benzene (2 mL), and pentane (20–25 mL) was added to precipitate a purple impurity. This mixture was filtered through Celite in a Kramer filter, and solvent was removed from the bright orange filtrate under oil pump vacuum. The resulting oil was dissolved in ether (2 mL), and pentane (20–25 mL) was added. Solvents were removed under oil pump vacuum to give (+)-(*R*)-**6a** as a light orange powder, mp 152–156 °C dec, $[\alpha]^{25}_{589}$ 388 ± 3°.[15]

Preparation of $(\eta^5\text{-}C_5H_5)Re(NO)(PPh_3)(OCH_2CH_2CH_3)$ (6b). A. Complex (*RS*,*SR*)-**3b**$^+BF_4^-$ (0.176 g, 0.255 mmol) and **5** (0.146 g, 0.255 mmol) were combined in a procedure analogous to that given for **6a**. An identical workup gave **6b** (0.139 g, 0.231 mmol, 91%) as a red-orange foam/oil, which dissolved in benzene (2.5 mL). Hexane (30 mL) was added, and the sample was taken to dryness under oil pump vacuum to give **6b** as a dark orange powder, mp 182–183 °C dec. Anal. Calcd for $C_{26}H_{27}NO_2PRe$: C, 51.82; H, 4.52. Found: C, 51.67; H, 4.55. Crystallization as with **6a** gave **6b** as ruby red rosettes, mp 183–185 °C dec. Anal. Found: C, 51.95; H, 4.53. B. Complex (+)-(*RS*)-**3b**$^+BF_4^-$ (0.103 g, 0.150 mmol) and **5** (0.083 g, 0.145 mmol) were reacted in a procedure analogous to that given for (+)-(*R*)-**6a**. This gave (+)-(*R*)-**6b** (0.079 g, 0.131 mmol, 90%) as a red-orange foam/oil, which was similarly converted to a dark orange powder, mp 181–183 °C dec, $[\alpha]^{25}_{589}$ 328 ± 2°.[15] Anal. Found: C, 51.27; H, 4.76.

Preparation of $(\eta^5\text{-}C_5H_5)Re(NO)(PPh_3)(OCH_2CH_2CH_2CH_3)$ (6c). A. Complex (*RS*,*SR*)-**3c**$^+BF_4^-$ (0.137 g, 0.195 mmol) and **5** (0.111 g, 0.193 mmol) were combined in a procedure analogous to that given for **6a**. An identical workup gave **6c** (0.102 g, 0.165 mmol, 86%) as a red-orange oil, which was dissolved in benzene (1 mL). Hexane was added, and the sample was concentrated under oil pump vacuum. Additional hexane was added, and the sample was taken to dryness to give **6c** as an orange powder, mp 162–164 °C, dec. Anal. Calcd for $C_{27}H_{29}NO_2PRe$: C, 52.58; H, 4.74. Found: C, 53.11; H, 4.69. Crystallization as with **6a** gave **6c** as ruby red rosettes, mp 164–166 °C dec. Anal. Found: C, 52.67; H, 4.75. B. Complex (+)-(*RS*)-**3c**$^+BF_4^-$ (0.106 g, 0.150 mmol) and **5** (0.083 g, 0.145 mmol) were reacted in a procedure analogous to that given for (+)-(*R*)-**6a**. This gave (+)-(*R*)-**6c** (0.078 g, 0.126 mmol, 87%) as a red-orange powder, which was reprecipitated as with (+)-(*R*)-**6a** to give a light orange powder, mp 163–169 °C dec, $[\alpha]^{25}_{589}$ 349 ± 2°.[15] Anal. Found: C, 52.67; H, 4.77.

Preparation of $(\eta^5\text{-}C_5H_5)Re(NO)(PPh_3)(OCH_2CH(CH_3)_2)$ (6d). A. Complex (*RS*,*SR*)-**3d**$^+BF_4^-$ (0.157 g, 0.224 mmol) and **5** (0.127 g, 0.221 mmol) were combined in a procedure analogous to that given for **6a**. An identical workup gave **6d** (0.109 g, 0.177 mmol, 80%) as a red-orange foam/oil, which was dissolved in benzene (1.4 mL). Pentane was added (15 mL), and the sample was taken to dryness under oil pump vacuum to give **6d** as an orange powder, mp 149–153 °C dec. Anal. Calcd for $C_{27}H_{29}NO_2PRe$: C, 52.58; H, 4.74. Found: C, 53.10; H, 4.81. Crystallization as with **6a** gave **6d** as ruby red rosettes, mp 156–158 °C dec. B. Complex (+)-(*RS*)-**3d**$^+BF_4^-$ (0.109 g, 0.155 mmol) and **5** (0.083 g,

(46) Brown, H. C. *Organic Syntheses via Boranes*; Wiley: New York, 1975; Figure 9.26; Aldrich Catalog No. Z10,139-7.

0.145 mmol) were reacted in a procedure analogous to that given for (+)-(*R*)-**6a**. This gave (+)-(*R*)-**6d** (0.078 g, 0.127 mmol, 87%) as a red-orange foam/oil, which was similarly converted to a dark orange waxy solid, mp 58–62 °C, $[\alpha]^{25}_{589}$ 394 ± 1°.[15] Anal. Found: C, 52.41; H, 4.75.

Preparation of (η^5-C_5H_5)Re(NO)(PPh$_3$)(OCH$_2$C$_6$H$_5$) (6e). A. Complex (*RS*,*SR*)-**3e**$^+$BF$_4^-$ (0.131 g, 0.177 mmol) and **5** (0.100 g, 0.174 mmol) were combined in a procedure analogous to that given for **6a**. An identical workup gave **6e** (0.108 g, 0.166 mmol, 95%) as a red foam/oil, which was dissolved in benzene (1 mL). Hexane (5 mL) was added (effecting some precipitation), and the sample was taken to dryness under oil pump vacuum to give **6e** (0.090 g, 0.138 mmol, 79%) as an orange powder, mp 171–173 °C dec. Anal. Calcd for $C_{30}H_{27}NO_2PRe$: C, 55.37; H, 4.18. Found: C, 55.46; H, 4.23. Crystallization as with **6a** gave **6e** as ruby red rosettes, mp 171–173 °C dec. Anal. Found: C, 55.31; H, 4.21. B. Complex (+)-(*RS*)-**3e**$^+$BF$_4^-$ (0.144 g, 0.196 mmol) and **5** (0.106 g, 0.185 mmol) were reacted in a procedure analogous to that given for (+)-(*R*)-**6a**. This gave (+)-(*R*)-**6e** (0.101 g, 0.156 mmol, 84%) as a red-orange powder, mp 174–176 °C dec, $[\alpha]^{25}_{589}$ 335 ± 2°.[15] Anal. Found: C, 55.42; H, 4.22.

Preparation of (η^5-C_5H_5)Re(NO)(PPh$_3$)(OCH$_2$CH$_2$C$_6$H$_5$) (6f). A. Complex (*RS*,*SR*)-**3f**$^+$BF$_4^-$ (0.150 g, 0.200 mmol) and **5** (0.111 g, 0.194 mmol) were combined in a procedure analogous to that given for **6a**. An identical workup gave **6f** as a red-orange oil, which was dissolved in benzene (2 mL). Hexane (4 mL) was added, and the sample was taken to dryness under oil pump vacuum to give **6f** (0.117 g, 0.176 mmol, 91%) as a red-orange powder, mp 152–157 °C dec. Anal. Calcd for $C_{31}H_{29}NO_2PRe$: C, 56.01; H, 4.40. Found: C, 56.11; H, 4.42. Crystallization as with **6a** gave **6f** as ruby red rosettes, mp 154–160 °C dec. Found: C, 56.13; H, 4.44. B. Complex (+)-(*RS*)-**3f**$^+$BF$_4^-$ (0.109 g, 0.145 mmol) and **5** (0.082 g, 0.143 mmol) were reacted in a procedure analogous to that given for (+)-(*R*)-**6a**. This gave (+)-(*R*)-**6f** (0.091 g, 0.136 mmol, 95%) as a dark orange oily solid, which was reprecipitated as with (+)-(*R*)-**6a** to give a dark orange waxy solid, mp 54–63 °C, $[\alpha]^{25}_{589}$ 331 ± 1°.[15] Anal. Found: C, 55.46; H, 4.75.

Reaction of (+)-(*R*)-6e and HI. A Schlenk tube was charged with (+)-(*R*)-**6e** (0.054 g, 0.083 mmol) and a stir bar and was cooled to −80 °C. Then CH_2Cl_2 (3 mL) and (after 10 min) HI (47% aqueous; 0.026 mL, 0.164 mmol) were added. The sample was stirred for 30 min at −80 °C. The −80 °C bath was then replaced by a −45 °C bath. After 30 min, an aliquot was removed, diluted with hexane, and dried over K_2CO_3. Chiral HPLC analysis (J. T. Baker Chiracel OD) showed (+)-(*R*)-**6e** to be consumed and iodide complex product (+)-(*R*)-**8** to be of ≥99% ee. The sample was stirred for 4 h at −45 °C. Then dodecane was added (0.0090 g, 0.012 mL, 0.528 mmol), and GC analysis showed a 92 ± 4% yield of benzyl alcohol.[47] Then CH_2Cl_2 was added, and the mixture was dried over K_2CO_3. The sample was filtered, and hexane was added to the filtrate. Solvents were removed by rotary evaporation, and the resulting purple residue was dissolved in CH_2Cl_2 (ca. 10 mL) and the drying step was repeated. This gave (+)-(*R*)-**8** as a purple powder (0.055 g, 0.083 mmol, 99%; 87% ee by chiral HPLC), $[\alpha]^{25}_{589}$ 196 ± 5° (84 ± 2% ee) (lit.[17] $[\alpha]^{25}_{589}$ 233°).[15a]

Reaction of (+)-(*R*)-6e and (CH$_3$)$_3$SiI. A 5-mm NMR tube was charged with (+)-(*R*)-**6e** (0.031 g, 0.047 mmol), hexamethylbenzene standard (0.0055 g, 0.034 mmol), and C_6D_6 (0.6 mL) and was capped with a septum. Next (CH$_3$)$_3$SiI (0.006 mL, 0.044 mmol) was added in 0.002-mL portions. The orange solution turned purple. A ^{1}H NMR spectrum indicated the clean formation of (+)-(*R*)-**8** and benzyl trimethylsilyl ether (δ 4.56, 0.09)[47] in 90 ± 5% and 80 ± 5% yields vs the standard. The solution was filtered through Celite and diluted with CH_2Cl_2. Dodecane was added, and GC analysis verified the formation of benzyl trimethylsilyl ether (78 ± 2%)[47] and did not show other volatile products. Hexane (ca. 5 mL) was added, and the solution was concentrated by rotary evaporation until a purple powder had precipitated and a colorless supernatant (2–3 mL) remained. Then (+)-(*R*)-**8** (0.028 g, 0.042 mmol, 89%) was isolated as described in the preceding experiment, $[\alpha]^{25}_{589}$ 200 ± 2°.[15a]

Reaction of 6e and CH$_3$COI. A 5-mm NMR tube was charged with **6e** (0.031 g, 0.047 mmol) and CD_2Cl_2 (0.6 mL) and was capped with a septum. Next CH_3COI (0.008 mL, 0.097 mmol) was added by syringe. The orange solution immediately turned purple. A ^{1}H NMR spectrum indicated the clean formation of **8** and benzyl acetate (δ 5.09, 2.08).[47] Then CH_2Cl_2 was added, and the sample was filtered through silica with the aid of additional CH_2Cl_2. Dodecane (0.0073 g, 0.043 mmol) was added to the filtrate, and GC analysis[47] verified the presence of benzyl acetate (89 ± 1%). Solvent was removed from the filtrate by rotary evaporation. Then CH_2Cl_2 (2 mL) was added to the greenish-brown residue. This solution was layered with hexane. Purple crystals formed. The green supernatant was decanted and the crystals were washed with pentane and dried under vacuum to give **8** (0.019 g, 0.028 mmol, 60%).

Reaction of (+)-(*R*)-6e and (−)-(*R*)-*O*-Acetylmandelic Acid. A pear-shaped flask was charged with (+)-(*R*)-**6e** (0.098 g, 0.151 mmol), (−)-(*R*)-*O*-acetylmandelic acid (0.075 g, 0.386 mmol), DMAP (0.0020 g, 0.016 mmol), and a stir bar and was cooled to 0 °C. Then CH_2Cl_2 (3.0 mL) and DCC (0.420 mL, 1.0 M in CH_2Cl_2) were added. The clear solution quickly clouded and was stirred for 48 h, during which time the bath was allowed to warm to room temperature. Solvent was removed by rotary evaporation. The residue was extracted with benzene, leaving dicyclohexyl urea. The extract was chromatographed on silica gel (230–400 mesh, 15 g) with 5:35:60 (v/v/v) ethyl acetate/benzene/hexane (150 mL) and then 50:50 ethyl acetate/hexane. The fractions containing ester (*R*)-**10e** were best identified by capillary GC (retention time 5.24 min, 225 → 275 °C at 5 deg/min). Complex (+)-(*RR*)-(η^5-C_5H_5)Re(NO)(PPh$_3$)(O(C=O)CH(OAc)C$_6$H$_5$) ((+)-(*RR*)-**9**) subsequently eluted as an orange band. Concentration of the appropriate fractions yielded (*R*)-**10e** (0.043 g, 0.150 mmol, >99%; ^{1}H NMR (δ, C_6D_6) 6.08 (s, AcOC*H*), 4.96 (d, *J* = 12.5 Hz, OC*H*H′), 4.83 (d, *J* = 12.5 Hz, OCH*H*′)[47] as a pale yellow oil and (+)-(*RR*)-**9** as a red-orange solid (0.107 g, 0.145 mmol, 97%), mp 89–91 °C dec, $[\alpha]^{25}_{589}$ 361 ± 7°.[15] A ^{1}H NMR spectrum (C_6D_6) indicated a de of >99%. Anal. Calcd for $C_{33}H_{29}NO_5PRe$: C, 53.80; H, 3.97. Found (two preparations): C, 53.90, 53.88; H, 4.00, 4.00. IR (cm^{-1}, thin film/KBr): 1737/1740 (m, ν_{CO} acetate), 1683/1672 (vs, ν_{NO}), 1655/1648 (s, ν_{CO} ReOCO). ^{1}H NMR (δ, $CDCl_3/C_6D_6$): 6.96–7.43/6.97–7.48 (m, 20 H), 5.61/6.10 (s, OCH), 5.11/4.90 (s, C_5H_5), 2.07/1.76 (s, CH_3). ^{13}C{^{1}H} NMR (ppm, $CDCl_3$): 176.2 (d, J_{CP} = 4.5 Hz, ReOCO), 169.9 (s, O_2CCH_3), 137.2 (s, CPh ipso), 133.9 (d, J_{CP} = 53.0 Hz, PPh ipso), 133.6 (d, J_{CP} = 11.3 Hz, PPh *o*), 130.4 (d, J_{CP} = 2.3 Hz, PPh *p*), 128.4 (d, J_{CP} = 10.8 Hz, PPh *m*), 128.0 (s, CPh), 127.6 (s, CPh), 127.4 (s, CPh), 90.7 (d, J_{CP} = 2.3 Hz, C_5H_5), 74.6 (s, OCH), 21.2 (s, CH_3). ^{31}P{^{1}H} NMR (ppm, $CDCl_3$): 20.7 (s).

Reaction of (+)-(*R*)-6e and (+)-(*S*)-*O*-Acetylmandelic Acid. A pear-shaped flask was charged with (+)-(*R*)-**6e** (0.078 g, 0.120 mmol), (+)-(*S*)-*O*-acetylmandelic acid (0.058 g, 0.297 mmol, 95.3% ee), DMAP (0.0011 g, 0.009 mmol), and a stir bar and was cooled to 0 °C. Then CH_2Cl_2 (1.0 mL) and DCC (0.240 mL, 1.0 M in CH_2Cl_2) were added. The reaction was conducted and worked up as in the preceding experiment to give (*S*)-**10e** (0.034 g, 0.118 mmol, 99%) as a pale yellow oil and (+)-(*RS*)-**9** as an orange powder (0.079 g, 0.108 mmol, 89%), mp 189–191 °C dec, $[\alpha]^{25}_{589}$ 340 ± 5°.[15] A ^{1}H NMR spectrum (C_6D_6) showed only traces of diastereomer (+)-(*RR*)-**9**. Anal. Calcd for $C_{33}H_{29}NO_5PRe$: C, 53.80; H, 3.97. Found: C, 53.74; H, 3.98. IR (cm^{-1}, thin film/KBr): 1738/1734 (m, ν_{CO} acetate), 1682/1687 (vs, ν_{NO}), 1656/1649, 1635 (s, ν_{CO} ReOCO; solid-state splitting). ^{1}H NMR (δ, $CDCl_3/C_6D_6$): 7.05–7.43/6.99–7.49 (m, 20 H), 5.61/6.01 (s, OCH), 5.26/5.00 (s, C_5H_5), 2.07/1.82 (s, CH_3). ^{13}C{^{1}H} NMR (ppm, $CDCl_3$): 176.0 (d, J_{CP} = 3.8 Hz, ReOCO), 170.3 (s, O_2CCH_3), 136.2 (s, CPh ipso), 133.8 (d, J_{CP} = 52.1 Hz, PPh ipso), 133.6 (d, J_{CP} = 11.3 Hz, PPh *o*), 130.3 (d, J_{CP} = 2.1 Hz, PPh *p*), 128.4 (d, J_{CP} = 10.4 Hz, PPh *m*), 128.0 (s, CPh), 127.6 (s, CPh), 127.2 (s, CPh), 90.7 (s, C_5H_5), 75.0 (s, OCH), 21.2 (s, CH_3). ^{31}P{^{1}H} (ppm, $CDCl_3$): 20.2 (s).

Reaction of (+)-(*R*)-6e, HBF$_4$·O(C$_2$H$_5$)$_2$, and Benzaldehyde. A Schlenk flask was charged with (+)-(*R*)-**6e** (0.074 g, 0.113 mmol), CH_2Cl_2 (3 mL), and a stir bar and was cooled to −80 °C. Then HBF$_4$·O(C$_2$H$_5$)$_2$ (0.019 mL, 0.12 mmol) was added by syringe with stirring. After 5 min, benzaldehyde (0.058 mL, 0.57 mmol) was added. The solution was allowed to warm to room temperature over the course of 3 h and kept at room temperature for 2 h. The solution was then cooled to 0 °C, and after 12 h ether (9 mL) was added. A precipitate formed, which was collected by filtration, washed with ether, and dried in vacuo (56 °C) to give (+)-(*RS*)-**3e**$^+$BF$_4^-$ as a bright yellow powder (0.068 g, 0.093 mmol, 82%), $[\alpha]^{25}_{589}$ 314 ± 2°.[15] Dodecane (0.0147 g, 0.0863 mmol) was added to the filtrate, and GC analysis[47] indicated the presence of benzyl alcohol (72 ± 5%).

Preparation of (η^5-C_5H_5)Re(NO)(PPh$_3$)(CDO) (5-*d*$_1$). A Schlenk flask was charged with [(η^5-C_5H_5)Re(NO)(PPh$_3$)(CO)]$^+$BF$_4^-$ (2.321 g, 3.52 mmol) and a stir bar. Deoxygenated THF and D_2O (56 mL, 1:1 v/v; 99.9% labeled)[48] were added, and the resulting suspension was cooled to 0 °C. Then a solution of $NaBD_4$ (0.234 g, 5.58 mmol, 98.8% labeled) in D_2O (2.0 mL) was slowly added dropwise. The yellow suspension was allowed to warm to room temperature and was stirred for 30 min. The solvents were concentrated under vacuum until the mixture became viscous. The mixture was extracted with CH_2Cl_2 (1 × 15 mL, 2 × 2.5 mL). The organic (lower) phases were separated by cannula and filtered

(47) These data were identical with those of an authentic sample.

(48) Substitution of D_2O by H_2O gave **5**-*d*$_1$ that was only ca. 90% labeled.

through a Celite/$MgSO_4$ column (4 cm, 1:1). The filtrate was collected in a Schlenk flask, and solvent was removed under vacuum. The resulting solid was dissolved in THF (55 mL) and layered with hexane (55 mL). Box-shaped amber crystals slowly formed. After 4 days, the supernatant was removed by cannula, and the crystals were washed once with hexane and dried under vacuum to give **5**-d_1 (1.111 g; corrected yield 1.89 mmol, 54%) that ^1H NMR analysis showed to contain 2.7 mol % (2.6 wt %) of trideuteriomethyl complex $(\eta^5\text{-}C_5H_5)Re(NO)(PPh_3)(CD_3)$ (**1**-d_3). The relative heights of the residual CHO and cyclopentadienyl ^1H NMR resonances were carefully measured (16 scans, 15-s delay) and calibrated to those of undeuterated **5** under identical conditions. These data showed **5**-d_1 to be 99.3% deuterated.[49] ^1H NMR (δ, $CDCl_3$): 16.53 (s, residual HCO), 7.36–7.44 (m, 15 H, 3 C_6H_5), 5.24 (s, C_5H_5). $^{13}C\{^1H\}$ NMR (ppm, $CDCl_3$): 252.2 (td, J_{CD} = 22.2 Hz, J_{CP} = 9.8 Hz, CDO), 135.1 (d, J_{CP} = 55.5 Hz, ipso), 133.0 (d, J_{CP} = 11.0 Hz), 130.4 (d, J_{CP} = 2.6 Hz, *p*), 128.4 (d, J_{CP} = 10.8 Hz), 93.5 (s, C_5H_5). $^{31}P\{^1H\}$ NMR (ppm, THF): 18.8 (s).

Preparation of (+)-(*S*)-$(\eta^5\text{-}C_5H_5)$Re(NO)(PPh$_3$)(CDO) ((+)-(*S*)-5-d_1). Complex (+)-(*S*)-$[(\eta^5\text{-}C_5H_5)Re(NO)(PPh_3)(CO)]^+BF_4^-$ (1.401 g, 2.13 mmol),[8] THF/D_2O (28 mL), and $NaBD_4$ (0.137 g, 3.27 mmol) in D_2O (1.5 mL) were combined in a procedure analogous to that given for **5**-d_1. The reaction mixture (which became homogeneous at room temperature) was concentrated, extracted with CH_2Cl_2 (1 × 10 mL, 2 × 5 mL), and filtered through Celite/$MgSO_4$ as above. The solvent was removed from the filtrate under vacuum to give a yellow-orange solid. The solid was dissolved in THF (5 mL), and hexane (10 mL) was slowly added with stirring. After 10 min, the resulting yellow powder was transferred by cannula to a Kramer filter, utilizing a hexane (10 mL) rinse.[50] The powder was dried under vacuum to give (+)-(*S*)-**5**-d_1 (0.949 g; corrected yield 1.58 mmol, 74%) that ^1H NMR analysis showed to contain 4.7 mol % (4.6 wt %) of (+)-(*S*)-**1**-d_3. Assay as above showed (+)-(*S*)-**5**-d_1 to be 99.1% deuterated.

Preparation of (*RR*,*SS*)-$(\eta^5\text{-}C_5H_5)$Re(NO)(PPh$_3$)(OCHDR) ((*RR*,*SS*)-6-d_1). A. A Schlenk tube was charged with (*RS*,*SR*)-**3a**$^+BF_4^-$ (0.1001 g, 0.148 mmol) and a stir bar. Then CH_2Cl_2 (3 mL) was added, and the tube was cooled to −80 °C. A solution of deuterioformyl complex **5**-d_1 (0.0866 g, corrected for 0.6 wt % **1**-d_3; 0.151 mmol) in CH_2Cl_2 (2 mL; then 1 mL rinse) was slowly added down the wall of the tube by cannula. The resulting suspension was stirred at −80 °C for 22 h. Solvent was then removed by oil pump vacuum, and the residue was extracted with benzene (4 mL). The extract was passed through a 3-cm column of base treated Florisil, and the orange-red band was eluted with additional benzene (8 mL). Solvent was removed from the eluate under oil pump vacuum to give (*RR*,*SS*)-**6a**-d_1 (0.0717 g, corrected for 9.1 wt % **5**-d_1 and 3.9 wt % **1**-d_3; 0.122 mmol, 82%) as a red-orange foam/oil. B. Complexes (*RR*,*SS*)-**6b–f**-d_1 were identically prepared on 0.134–0.145-mmol scales utilizing 0.99–1.02 equiv of **5**-d_1 (86–99% yields after correction for 2–7 wt % impurities). NMR spectra were identical with those of optically active analogues below, and stereoselectivities are summarized in Scheme IV.

Preparation of (+)-(*RR*)-$(\eta^5\text{-}C_5H_5)$Re(NO)(PPh$_3$)(OCHDR) ((+)-(*RR*)-6-d_1). A. Complexes (+)-(*RS*)-**3a**$^+BF_4^-$ (0.1005 g, 0.149 mmol) and (+)-(*S*)-**5**-d_1 (0.0848 g, corrected for 4.6 wt % **1**-d_3; 0.148 mmol) were combined in a procedure analogous to that given for the racemates above. An identical workup gave (+)-(*RR*)-**6a**-d_1 (0.0772 g, corrected for 2.6 wt % **5**-d_1 and 5.8 wt % **1**-d_3; 0.131 mmol, 88%) as a red-orange foam/oil. B. Complexes (+)-(*RR*)-**6b–f**-d_1 were identically prepared on 0.133–0.148-mmol scales utilizing 1.00–0.93 equiv of (+)-(*S*)-**5**-d_1 or (−)-(*R*)-**5**-d_1 (68–99% corrected yields, 82–95% purities). Stereoselectivities are summarized in Scheme IV. C. Selected NMR data on (+)-(*RR*)-**6**-d_1: ^1H NMR (δ vs TMS, C_6D_6, C*H*D): **a**, 3.98 (q, J_{HH} = 7 Hz); **b**, 4.04 (t, J_{HH} = 6 Hz); **c**, 4.09 (t, J_{HH} = 6 Hz); **d**, 4.03 (d, J_{HH} = 6 Hz); **e**, 5.38 (br s); **f**, 4.32 (dd, J_{HH} = 5, 7 Hz). $^{13}C\{^1H\}$ NMR (ppm vs C_6D_6 at 128.0, C*H*D): **a**, 81.0 (td, J_{CD} = 21 Hz, J_{CP} = 7 Hz); **b**, 88.3 (td, J_{CD} = 21 Hz, J_{CP} = 6 Hz); **c**, 86.1 (br td, J_{CD} = 20 Hz, J_{CP} = 7 Hz); **d**, 94.2 (br td, J_{CD} = 21 Hz, J_{CP} = 6 Hz); **e**, 88.8 (br td, J_{CD} = 21 Hz, J_{CP} = 6 Hz); **4**, 88.1 (br td, J_{CD} = 21 Hz, J_{CP} = 5 Hz). Selected ^1H NMR data on (+)-(*RS*)-**6**-d_1 (C*H*D; minor diastereomers from preceding reactions): **a**, 4.22 (q, J_{HH} = 7 Hz); **b**, 3.95 (t, J_{HH} = 7 Hz); **c**, 3.97 (t, J_{HH} = 6 Hz); **d**, 3.59 (d, J_{HH} = 6 Hz); **e**, 4.94 (br s); **f**, 4.10 (br t, J_{HH} = 7 Hz).

Reactions of (*RR*,*SS*)-6-d_1 and (+)-(*RR*)-6-d_1 with (−)-(*R*)-*O*-Acetylmandelic Acid. These were conducted similarly to the reaction of (+)-(*R*)-**6e** and (−)-(*R*)-*O*-acetylmandelic acid described above. Representative run: (*RR*,*SS*)-**6a**, 0.0717 g, corrected for 3.9 wt % **5**-d_1 and 9.1 wt % **1**-d_3, 0.122 mmol; (−)-(*R*)-acetylmandelic acid, 0.0589 g, 0.303 mmol; DMAP, 0.0020 g, 0.016 mmol; DCC, 0.350 mL, 1.0 M in CH_2Cl_2; 18 h reaction time. After silica gel chromatography, the fractions containing (*RR*,*RS*)-**10a**-d_1 were concentrated and passed through a column of 2 cm of silica (bottom) and 2 cm of $AgNO_3$-treated silica (15% w/w, top) with 15:85 (v/v) ethyl acetate/hexane (15 mL). Solvent was removed from the eluate to give (*RR*,*RS*)-**10a**-d_1 (0.0234 g, 0.105 mmol, 86%) as a colorless oil. The fractions containing **9** were concentrated to give a red-orange solid. This was extracted with a minimum of benzene, leaving a white solid. The extract was concentrated to give **9** (0.084 g, 0.114 mmol, 94%) as a 50:50 mixture of (*RR*)/(*SR*) diastereomers.

Crystal Structure of (*RS*,*SR*)-3f$^+PF_6^-\cdot(CH_2Cl_2)_{0.5}$. A crystal was obtained as described above and mounted on a glass fiber. No symmetry was evident in axial photographs, indicating a triclinic lattice. Unit cell dimensions were obtained by least-squares refinement with use of 25 centered reflections for which $20° < 2\theta < 30°$. Data were collected on a Nicolet Re3/mE four-circle diffractometer as outlined in Table II. Azimuthal scan data were collected for 16 reflections at intervals of 15° in ϕ.

Data reduction[51] included corrections for Lorentz and polarization effects. Non-hydrogen atoms were refined with anisotropic thermal parameters by blocked cascade least-squares, minimizing $\sum w\Delta^2$, with 101 parameters in each full-matrix block. Difference electron density maps indicated a disordered CH_2Cl_2 molecule, which was modeled by fitting three orientations to the peak positions from difference maps. The PF_6^- anion was also disordered and was modeled with two orientations related by rotation about an F–P–F axis. The PF_6^- orientations were refined as rigid groups with anisotropic thermal parameters. The sum of the occupation factors was set to unity. The three orientations of the disordered CH_2Cl_2 were refined as rigid groups (hydrogen atoms not included) in two stages. First, isotropic thermal parameters were fixed and site occupation factors were refined. The combined occupation factors for the three orientations totaled 0.485. Second, CH_2Cl_2 site occupation factors were fixed and isotropic thermal parameters were refined. The following conditions were imposed during the final refinement cycles: hydrogen atoms were included in calculated positions; a common isotropic thermal parameter was refined for the phenyl hydrogens; other hydrogens were given thermal parameters fixed at 1.2 times the equivalent isotropic thermal parameters of their respective carbon atoms; the orientations used to model the disordered CH_2Cl_2 and PF_6^- were refined as rigid groups, with anisotropic thermal parameters refined for PF_6^- and isotropic refinement for CH_2Cl_2; and site occupation factors for CH_2Cl_2 and PF_6^- were constrained as described. Scattering factors were taken from the literature.[52] Empirical corrections for absorption were based on the azimuthal scan data with a transmission factor range of 0.63–0.98. Seven reflections showing strong extinction effects were excluded from the final refinement. The largest peaks of the final difference map were ca. 1.3 e/Å^3 and located ≤1 Å from the rhenium. Other peaks of about 1 e/Å^3 were found in the vicinity of the disordered CH_2Cl_2.

Crystal Structure of (*RS*,*SR*)-3b$^+BF_4^-$. A crystal was mounted as above. The unit cell determination, data collection, data reduction, and non-hydrogen atom location and refinement were conducted analogously. Absorption corrections were calculated by Gaussian integration with use of measured distances between indexed crystal faces (transmission range 0.139–0.309).

Refinement behavior and difference maps showed the BF_4^- anion and propionaldehyde methyl orientations to be disordered. The BF_4^- disorder was modeled by two fluorine orientations about a common boron. Angles in both were constrained to be tetrahedral, with all boron–fluorine distances refined by a common parameter. A common isotropic thermal parameter was refined for the boron atom and the eight partially occupied fluorine positions. The occupancy ratio for the two orientations refined to 55:45. The propionaldehyde methyl disorder was modeled with two orientations related by a rotation of ca. 110° around the C(1)–C(2) bond. Refinement behavior was improved by using two positions, 0.5 Å apart, for C(2). Propionaldehyde C–C distances were constrained to idealized values, and the C(1)–C(2)–C(3) angles for the two orientations were constrained to a common refined value. The occupancy ratio for the two orientations refined to 61:39. Calculated positions were used for all hydrogen atoms with a common refined isotropic thermal parameter. No corrections were made for extinction. The largest peaks of the final difference map were ca. 1.0 e/Å^3 and located near the BF_4^-, indicating

(49) As little as 0.2% of undeuterated **5** would have been observed. Hence, deuteration limits as high as ≥99.8% can be set by this method.

(50) The supernatant contained (+)-(*S*)-**5**-d_1 and (+)-(*S*)-**1**-d_3 in a ca. 1:1 ratio. Thus, the precipitation improved product purity.

(51) All crystallographic calculations were performed on a Data General Eclipse computer with the SHELXTL program package by G. M. Sheldrick, Nicolet Analytical Instruments, Madison, WI, 1983.

(52) Cromer, D. T.; Waber, J. T. In *International Tables for X-ray Crystallography*; Ibers, J. A., Hamilton, W. C., Eds.; Kynoch: Birmingham, England, 1974; Vol. IV, pp 72–98, 149–150.

the disorder model to be overly simplified.

Acknowledgment. We thank the NIH for support of this research and NRSA Postdoctoral Fellowships (C.M.G., J.J.K.) and K. Houk for the data in ref 33a.

Supplementary Material Available: Tables of atomic coordinates and anisotropic thermal parameters for (*RS,SR*)-**3b**$^+$$BF_4^-$ and (*RS,SR*)-**3f**$^+$$PF_6^-$·$(CH_2Cl_2)_{0.5}$ and NMR data for **10** (8 pages); table of calculated and observed structure factors for (*RS,SR*)-**3b**$^+$$BF_4^-$ (19 pages).[53] Ordering information is given on any current masthead page.

(53) Calculated and observed structure factors for (*RS,SR*)-**3f**$^+$$PF_6^-$·$(CH_2Cl_2)_{0.5}$ are given in the supplementary material in ref 12.

Multistep Electron Transfer in Palladium-Catalyzed Aerobic Oxidations via a Metal Macrocycle–Quinone System

Jan-E. Bäckvall,* R. Bruce Hopkins, Helena Grennberg, Mary M. Mader, and Alok K. Awasthi

Contribution from the Department of Organic Chemistry, University of Uppsala, Box 531, 751 21 Uppsala, Sweden. *Received December 29, 1989*

Abstract: Selective palladium-catalyzed aerobic conditions of olefins and conjugated dienes with the aid of a metal macrocycle–quinone system have been developed. This involves a multistep electron transfer with three catalysts ($Pd(OAc)_2$, hydroquinone, metal macrocycle). The triple catalytic system was applied to (i) 1,4-oxidation of conjugated dienes (1,4-diacetoxylation and 1,4-dialkoxylation), (ii) oxidation of terminal olefins to ketones, and (iii) allylic oxidation of cyclic olefins to 2-alken-1-yl acetates. The reactions occur under very mild conditions, (i) and (ii) at room temperature and (iii) at 60 °C, and are reminiscent of aerobic processes occurring in living organisms. Thus, there is an electron transfer from the substrate to Pd(II) giving Pd(0), followed by another electron transfer from Pd(0) to benzoquinone. The hydroquinone thus formed transfers electrons to the oxidized form of the metal macrocycle, which is reduced. The latter is reoxidized by electron transfer to molecular oxygen. A number of metal macrocycles such as metal(salen) complexes Co(salophen), Co(TPP), and iron phthalocyanine (Fe(Pc)) were tested as oxygen-activating complexes. In the 1,4-diacetoxylation of 1,3-dienes, and in the allylic oxidation, several of these metal macrocycles gave good results. In the 1,4-dialkoxylation of 1,3-dienes and in the oxidation of terminal olefins to ketones, which occur in the presence of a strong acid, only Fe(Pc) survived the reaction conditions.

Metal-catalyzed oxidation of organic compounds is an expanding area of organic chemistry with many applications in industrial processes.[1,2] Today there is an increasing need for mild aerobic catalytic processes due to energy saving and environmental reasons. Most of the known oxidation processes based on molecular oxygen, however, require elevated temperature and pressure.

Recently, macrocyclic metal complexes, in particular metalloporphyrins, have attracted attenation as catalysts in oxidation reactions.[3-9] Most of the metalloporphyrins used have utilized oxidants such as iodosylbenzene,[4] hypochlorite,[5] persulfate,[6] and peroxide.[7] There are only a few examples[8,9] of the use of molecular oxygen as the ultimate oxidant, and in these systems, except in a few,[8c,9] a reductive activation of oxygen is needed. We have been engaged in palladium-catalyzed oxidation of olefins and conjugated dienes and have developed a number of selective reactions.[9-12] Recently we were able to develop procedures that allow an aerobic oxidation via a multistep electron transfer involving three redox systems Pd(II)/Pd(0)–benzoquinone/hydroquinone–ML^m_{ox}/ML^m, where ML^m is an oxygen activating macrocyclic transition metal complex.[9] In this paper we give a full account of this remarkably mild triple catalytic system. It has been applied to three principal types of reactions: (i) oxidation

Scheme I

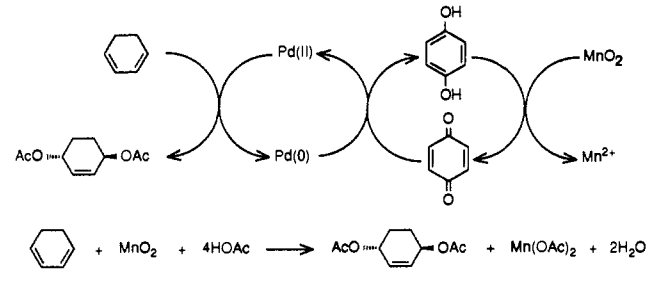

(1) (a) Sheldon, R. A.; Kochi, J. K. *Metal-Catalyzed Oxidations of Organic Compounds*; Academic Press: New York, 1981.
(2) Parshall, G. W. *Homogeneous Catalysis*; Wiley-Interscience: New York, 1980.
(3) For a review, see: Meunier, B. *Bull. Soc. Chim. Fr.* **1986**, 578.
(4) (a) Groves, J. T.; Nemo, T. E.; Myers, R. S. *J. Am. Chem. Soc.* **1979**, *101*, 1032. (b) Groves, J. T.; Kruper, W. J.; Haushalter, R. S. *Ibid.* **1980**, *102*, 6375. (c) Hill, C. L.; Schardt, J. A. *Ibid.* **1980**, *102*, 6374.
(5) (a) Guilmet, E.; Meunier, B. *Tetrahedron Lett.* **1980**, *21*, 4449. (b) De Carvalo, M. E.; Meunier, B. *Tetrahedron Lett.* **1983**, *24*, 3621.
(6) De Poorter, B.; Ricci, M.; Meunier, B. *Tetrahedron Lett.* **1985**, *26*, 4459.
(7) (a) Renaud, J. P.; Battioni, P.; Bartoli, J. F.; Mansuy, D. *J. Chem. Soc., Chem. Commun.* **1985**, 888. (b) Mansuy, D.; Bartoli, J. F.; Momenteau, M. *Tetrahedron Lett.* **1982**, *23*, 2781.
(8) (a) Tabushi, I.; Koga, N. *J. Am. Chem. Soc.* **1979**, *101*, 6456. (b) Perrée-Fauvet, M.; Gaudemer, A. *J. Chem. Soc., Chem. Commun.* **1981**, 874. (c) Groves, J. T.; Quinn, R. *J. Am. Chem. Soc.* **1985**, *107*, 5790. (d) Tabushi, I.; Morimitsu, K. *Ibid.* **1984**, *106*, 6871. (e) Mansuy, D.; Fontecave, M.; Bartoli, J. F. *J. Chem. Soc., Chem. Commun.* **1983**, 253.
(9) (a) Bäckvall, J. E.; Awasthi, A. K.; Renko, Z. D. *J. Am. Chem. Soc.* **1987**, *109*, 4750. (b) Bäckvall, J. E.; Hopkins, R. B. *Tetrahedron Lett.* **1988**, *29*, 2885.
(10) (a) Bäckvall, J. E.; Nyström, J. E.; Nordberg, R. E. *J. Am. Chem. Soc.* **1985**, *107*, 3676. (b) Bäckvall, J. E.; Granberg, K. L.; Hopkins, R. B. *Acta Chem. Scand.* In press.
(11) (a) Bäckvall, J. E.; Byström, S. E.; Nordberg, R. E. *J. Org. Chem.* **1984**, *49*, 4619. (b) Bäckvall, J. E.; Vågberg, J.; Nordberg, R. E.; *Tetrahedron Lett.* **1984**, *25*, 2717.
(12) Bäckvall, J. E.; Vågberg, J. O. *J. Org. Chem.* **1988**, *53*, 5695.

0002-7863/90/1512-5160$02.50/0